Probing the nature and reactivity of coordination complexes with blended organic and inorganic chromophores using vibrational spectroscopy

Raphael Horvath,[a] Gregory S. Huff,[b] Keith C. Gordon[b,*] and Michael W George[a,c*]

a School of Chemistry, University of Nottingham, School of Chemistry, Nottingham, UNG7 2RD, UK

b University of Otago, Department of Chemistry, PO Box 56, Dunedin, New Zealand

c Department of Chemical and Environmental Engineering, The University of Nottingham Ningbo China, Ningbo, 315100, China

Table of Contents

1 Abstract

The use of transient vibrational spectroscopy in the analysis of rhenium(I) and ruthenium(II) complexes is discussed. Particular focus is given to the use resonance Raman spectroscopy to probe initial photoexcitation and transient resonance Raman and infrared spectroscopy to observe subsequent relaxation processes. The utility of these techniques is given by discussion of examples in which the electronic complexity of the system increases from systems which are nominally *pure* metal-to-ligand charge-transfer through to systems which have complex interplay between intraligand and metal-to-ligand charge transfer states. The use of these later systems in dye-sensitised solar cells is also briefly discussed.

2 Introduction

Metal polypyridyl complexes have found utility across a range of applications that include: solar cells [1, 2]; sensors[3-5]; organic light-emitting diodes[6-9]; photocatalysis.[10-13] In all of these applications the excited state is one of the key species that facilitates the desired properties.

In this review we discuss charge-transfer states associated with metal systems (almost exclusively Re(I) and Ru(II)). We begin by focusing on systems where the lowest excited state may be described as metal-to-ligand charge-transfer (MLCT) or more precisely, systems with ligands that are involved in a clearly identifiable MLCT transition. We then describe coordination complexes in which ligands offer a number of closely lying excited states such as MLCT and ligand centered (LC) π,π^*. We illustrate with exemplarily systems involving complexes of the dipyrido[3,2-a:2’,3’-c]phenazine (dppz) ligand. Finally we focus on systems in which the ligands have been deliberately designed to include intra-ligand charge-

transfer (ILCT) or additional low energy transitions. These have found considerable use in solar cell applications and we provide a section dedicated to that utility.

Vibrational spectroscopy is a useful method of understanding excited state properties. Focus is given here to the use of resonance Raman spectroscopy, time-resolved infrared and transient resonance Raman spectroscopy (including time-resolved resonance Raman).

A comprehensive review of the analysis and characterization of coordination compounds using resonance Raman techniques (including time-resolved methods) has been published. [14] In an attempt to avoid repetition we focus on exemplar studies, in a number of cases post 2011, in which the structure of the excited states has been elucidated.

2.1 FC and THEXI states

A variety of spectroscopic methods may be brought to bear on the interrogation of excited state properties. It is useful to distinguish between two types of excited state that are being examined (Figure 1). In electronic absorption and resonance Raman spectroscopy the excited state surface being probed has the ground state nuclear coordinates and is termed the Franck-Condon (FC) state. For time-resolved methods such as transient absorption, time-resolved infrared (TRIR) and resonance Raman the thermally equilibrated excited (THEXI) state may be examined. This is an important differentiation in inorganic systems because the nature of the FC state is normally singlet and the THEXI state is almost always triplet. Furthermore the quantum yield for intersystem crossing is close to unity.[15]

In discussing the complexes in this review each has been classified as possessing conventional MLCT, mixed MLCT, LC π,π^* or engineered multichromophores. This classification is based on the ligand and is somewhat arbitrary. It does, however, separate the systems discussed on the basis of their electronic structure complexity and provides some order to the presentation of these data.

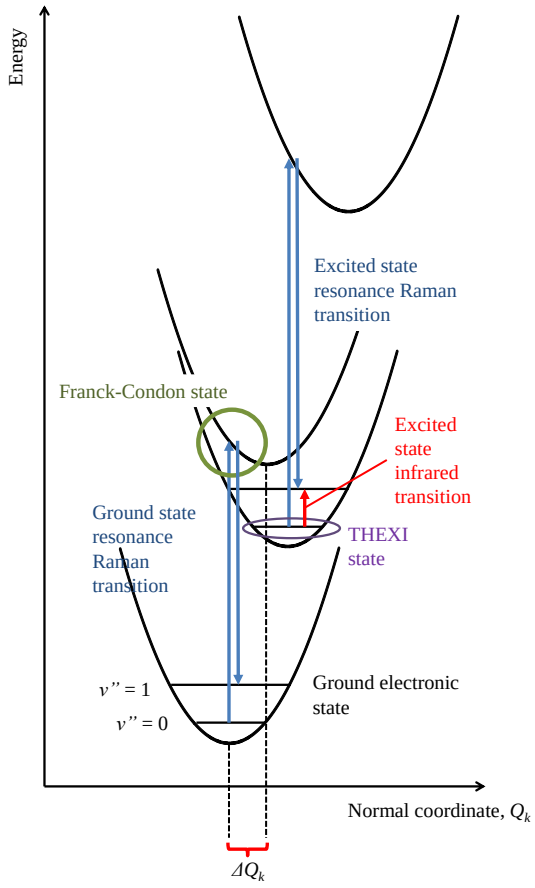

Figure 1. Depiction of ground and excited state surface energies, as a function of normal coordinate Q_k, probed by resonance Raman spectroscopy, ground state and excited state, (Stokes scattering) and time-resolved infrared spectroscopy.

2.2 MLCT states

The MLCT state involves the photoexcitation from a metal dπ orbital to a ligand π* orbital. Thus the metal is formally oxidised and the ligand reduced. This type of excited state has predictable behaviour because of the inter-relation of properties (such as transition intensity (oscillator strength), lifetime and quantum yield, transition energy) with the energies and respective displacements (ΔQ_k) of the potential energy surfaces.

One of the early descriptions of a metal-to-ligand charge-transfer system is {$Re(CO)_3X(N\hat{}N)$}, where (N^N) is a bidentate dimmine ligand, This exemplifies some of the properties that make these systems so interesting.[16] In this study the emission properties of the $Re(CO)_3Cl(phen)$ and $[Re(CO)_3X(phen)]^+$ (where X = pyridine, piperidine, PhCN, CH_3CN) are reported. The ancillary ligand modulates the electron density at the metal which can be followed by examination of the $\tilde{\nu}$(CO) wavenumbers. The complex with the highest $\tilde{\nu}$(CO) has the lowest electron density at the metal resulting in a higher energy MLCT band.

The energy of the MLCT transition may also be guided by substituents on the dimminett ligand. An early study on $Ru(bpyX_2)_3^{2+}$ systems showed a linear relationship between emission energy and difference between electrochemical potentials for first oxidation and first reduction ($E_{½}$).[17] Furthermore the $E_{½}$ showed a linear relationship to the Hammett σ constants for the substituents.

In a detailed study of the photophysics of a series of $Re(CO)_3Cl(bpyX_2)$ Worl et al.[18] showed that $E_{½}$was linearly related to both emission and absorption bands for the MLCT state. Furthermore the distortion of the excited state from the ground state (ΔQ_k in Figure 1) could be determined via analysis of the emission profile and showed a linear correlation with the emission energy; finally they were able to show that the non-radiative decay (which dominates the lifetime of the excited state) was related to the Franck-Condon factors that could be extracted via resonance Raman excitation profile measurements (vide infra) or emission band-fitting. The upshot of this was that it is possible to predict dynamic properties based on fairly simple design principles associated with energetics and, for a series of related compounds, Hammett constants. The understanding of these processes was exploited to create long-lived low energy MLCT states by using ligands which delocalised charge and thus had relatively small ΔQ.[19, 20]

2.3 MLCT and LC states

An exemplar of a multiple excited state complexes are those that involve the ligand dipyrido[3,2-a:2',3'-c]phenazine (dppz, see Figure 2). This is because the LC and MLCT states lie at similar energies (indeed there are two differing MLCT states close in energy). Complexes of dppz have been studied with respect to use in solar cell devices [21-23] and have been used in organic light emitting diodes.[24-29] However, most prominently, it is known to undergo the light-switch effect, whereby the complexes are non-emissive in aqueous solutions and become emissive in organic solvents or in the presence of DNA.[30-39] This provides a number of interesting potential uses, including biosensing and DNA cleavage (*vide infra*).

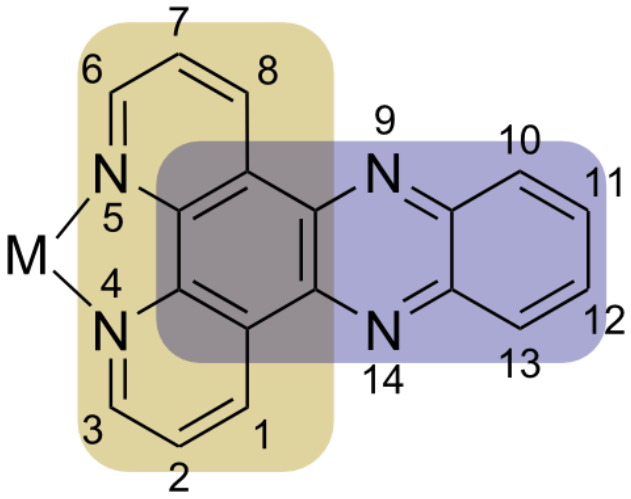

Figure 2. The metal-coordinated dppz ligand, showing the locations of the phenanthoroline-like (yellow) and phenazine-like (blue) molecular orbitals and the numbering scheme for substitution.

The origin of the interesting and complex behavior exhibited by the complexes of dppz is the presence of several close-lying unoccupied molecular orbitals (MOs). When chelated to a closed-shell metal such as Ru^{2+} or Re^{+} this results in two close-lying metal to ligand charge transfer (MLCT) states as well as several possible ligand-centered $\pi \rightarrow \pi^*$ states. Population of the MO on the phenanthroline-like (phen) portion of the ligand involves overlap of electron density with the chelating nitrogen atoms, while population of the MO on the phenazine-like (phz) portion of the ligand shifts electron density away from the metal. The resulting MLCT(phen) and MLCT(phz) states possess different properties (e.g. luminescence). These as well as several LC states have been identified using transient Raman and TRIR spectroscopic techniques and their interplay can be tuned by various substitution patterns on the dppz ligand and modification of the ancillary ligand (*vide infra*).[40-47]

3 Spectroscopic tools

3.1 Resonance Raman spectroscopy

One notable feature of resonance Raman spectroscopy is that it provides insight into the resonant transition.[48, 49] This is expressed by Tsuboi's rule, which states that if the excitation wavelength is chosen to coincide with an electronic transition then vibrational bands will be enhanced in intensity if the vibrations mimic the structural distortion upon photoexcitation.[50, 51] As structural distortion is related to the movement of electrons, empirical use of this relationship can be made to determine the donor/acceptor regions involved in an excited state.

Resonance Raman spectroscopy has been used to probe MLCT transitions at a number of levels. At its simplest it can be used to differentiate which ligand is the acceptor in an MLCT

transition for a heteroleptic system. This is shown in a study of Cu(I) complexes with dppz in which one ligand is dppz-based and the other bpy-based as shown in Figure 3.[52] At shorter excitation wavelengths the spectral features associated with dppz dominate, such as the band at 1401 cm^{-1}; this feature loses enhancement as the wavelength is tuned to the red where the Cu → bpy MLCT transition dominates. In turn the bpy modes at 1365 and 1489 cm^{-1} become more intense at these longer excitation wavelengths.

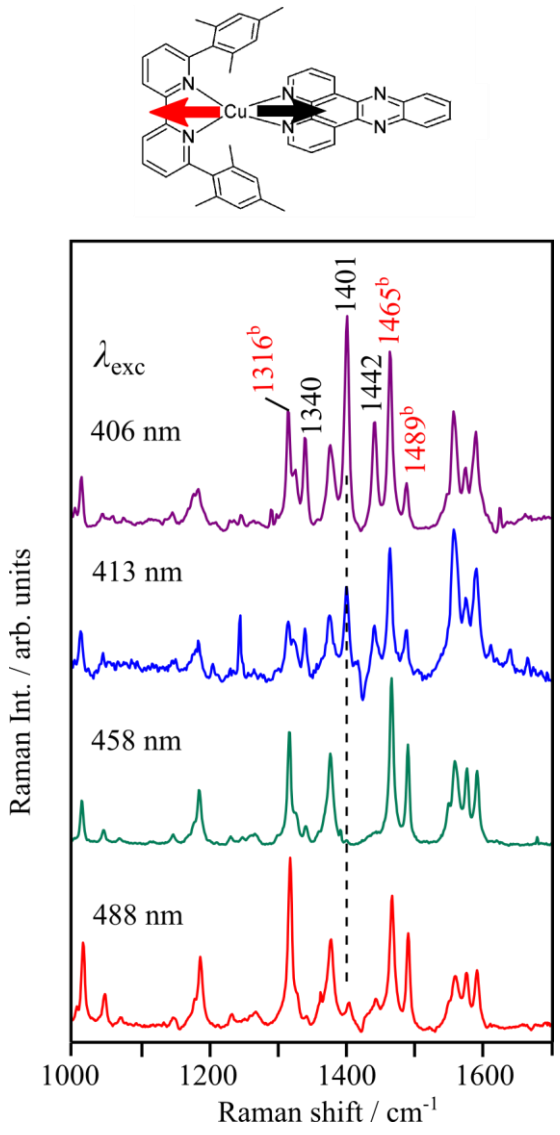

Figure 3. Resonance Raman spectra of $[Cu(bpy(Mes)_2)(dppz)]^+$ (CH_2Cl_2 solution). At short excitation wavelengths the Cu → dppz transition, black arrow, dominates; at longer excitation wavelengths the Cu → bpy transition, red arrow, dominates. Modes associated with boy are denoted by superscript b. [52]

It is also possible to use resonance Raman spectroscopy to determine the distortion between ground and resonant excited state through the construction of a resonance Raman excitation profile. This is because the resonance enhancement of band intensity is related to a number of factors including ΔQ (Figure 1) and the curvature of the normal mode of vibration (ω).[48]

Such measurements are uncommon in metal polypyridyl systems [53-57] for a number of reasons: firstly the large number of normal modes that exist in many polypyridyl systems can make unambiguous determination of structural changes challenging; secondly the advent of ultrafast lasers means that many spectroscopic techniques can actually time-resolve evolution from the FC state and this can be as informative as a resonance excitation profile study.[58, 59] Over the last few years accurate modelling of the resonance excitation profiles and resonance Raman spectra has been pioneered by the Guthmuller group. [60-74] The utility of resonance Raman spectral calculations and their success over such a range of compounds suggests that this area of research will grow.[75]

3.2 Time-resolved infrared spectroscopy

Time resolved infrared (TRIR) spectroscopy has proven useful in the identification and assignment of excited states. The techniques initially employed were nanosecond step-scan TRIR[76, 77], followed by ultrafast pump-probe experiments extending to the picosecond timescale.[78-81] Typically, for ultrafast pump-probe TRIR a seed laser is split to create two optically linked pulses, which are then amplified and converted to UV and IR wavelengths to serve as the pump and probe pulses respectively. The pump-probe time delay is adjusted via an optical delay line before the sample, and the probe pulse is analysed with a spectrograph and array detector. Non-consecutive pump pulses are removed, affording a pump-on/pump-off recording scheme, which allows for difference spectra to be generated, where an

individual background spectrum is subtracted for each "pump-on" spectrum. This means that only changes due to the photoexcitation are present as features in the resulting spectra.

Infrared reporter groups are often utilised, which are species with well-defined stretching frequencies in otherwise quiet parts of the spectral region; their shifts upon photoexcitation can be very diagnostic of particular types of excited states formed. Important reporter groups include organic and inorganic carbonyls, cyanide, thiocyanate and alkynes.[40, 41, 46, 76, 82-91] A prominent example is the carbonyl ligands of the [*fac*-$Re(CO)_3(L)(N\hat{}N)]^+$ fragment[51] (N^N = diimine; L = anion or py-derivative); the CO antibonding orbitals are electronically linked to the dπ(Re) orbitals and, by extension, to the diimine. Thus a change of electron density at the metal or on the ligand results in a change in $\tilde{\nu}$(CO), the direction and magnitude of which can be diagnostic of the nature of the electronic shifts. Furthermore the vibrational signature of the *fac*-$Re(CO)_3$ provides three well-defined vibrational modes. These are the symmetric stretch (termed a'(1)), which has the highest wavenumber, and two asymmetric stretches, one involving only the equatorial CO ligands (termed a") and the other all three (termed a'(2)). The ordering in terms of wavenumbers is $\tilde{\nu}_{a'(1)} > \tilde{\nu}_{a'(2)} > \tilde{\nu}_{a"}$ on going to the MLCT state as determined by Bredenbeck et al using 2D TRIR.[92] The nature of the lowest excited states of several dppz-complexes have been identified using TRIR spectroscopy on the picosecond timescale.[40-47, 93] This is well illustrated by the ps-TRIR spectra of $[Re(CO)_3Cl(dppz)]$ in C_3H_7CN (Figure 4) following excitation at 400 nm.[44] The initial red-shift of the a' CO band of 58 cm^{-1} is indicative of the formation of a MLCT(phen) state. Over the course of *ca.* 500 ps a second band forms, shifted by 69 cm^{-1}, which is consistent with the formation of an equilibrium of MLCT(phen) and MLCT(phz) states. An additional weak band, shifted by 6 cm^{-1} to lower energy is indicative of a $\pi \rightarrow \pi^*$ state. As discussed below, interplay between these states can be tuned by various substitution patterns on the dppz ligand and modification of the ancillary ligand.

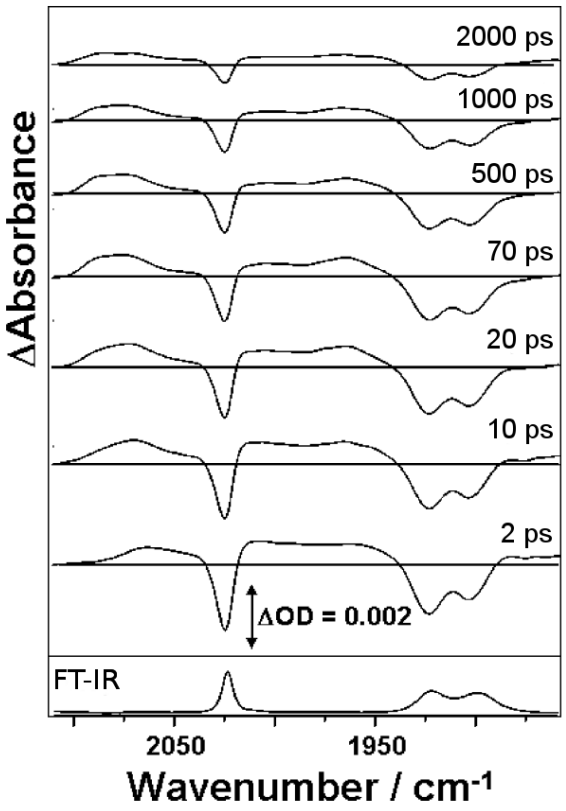

Figure 4. ps-TRIR spectra of $[Re(CO)_3Cl(dppz)]$ in C_3H_7CN at several time-delays after photoexcitation at 400 nm. Reprinted with permission from ref. [44]. Copyright (2008) American Chemical Society.

3.3 Transient Raman spectroscopy

It is possible to acquire Raman spectra of excited states. This is experimentally straightforward in that if a pulsed laser is used then the Raman scattering from the sample will be from the state that is populated during the duration of the laser pulse.[47, 94] If the excited state has a lifetime that is comparable or shorter than the laser pulse then the excited state features show a nonlinear intensity dependence with laser fluence. This is because one photon is needed to populate the excited state and the second to provide the resonance Raman scattering that is observed.[95, 96] If a single laser is used this is commonly referred to as a single-colour transient resonance Raman spectroscopy. In order to obtain reasonable data, in

general, the populated excited state must be in resonance and the ground state must be absorbing to populate the excited state. Many metal polypyridyl complexes meet this criterion as the electronic absorption of both ground and excited state are common. For excited state systems that have much longer lifetimes than the laser pulse it is possible to observe entirely excited state spectra.[25-27] This may be accomplished by using a mechanical chopper from a CW laser.[97] Early studies of metal polypyridyl complexes focused on charge localisation. Woodruff et al. showed that the formulation for the MLCT excited state of $[Ru(bpy)_3]^{2+}$ was localised on a single ligand by comparison of the transient resonance Raman spectrum with chemically prepared $bpy^{\cdot-}$.[98, 99] Some care is required in the use of the single-colour experiment. The limitation of requiring absorption from the ground and excited state means that there is no control over what chromophore of the excited state is being probed. In the case of $[Ru(bpy)_3]^{2+}$ the success of the experiment hinged on the fact that $bpy^{\cdot-}$ absorbs strongly at 355 nm. It is interesting to note that the other major chromophore in the MLCT state of $[Ru(bpy)_3]^{2+}$ is the LMCT bpy $\rightarrow$ Ru(III) which shows spectral signatures almost identical to the ground state.[98, 99] This is not the case for $[Ru(phen)_3]^{2+}$ and the transient resonance Raman of this system has proven to be controversial in its interpretation in part because of the poor absorption of $phen^{\cdot-}$ at 355 nm.[100-102] An additional limitation of single-colour transient resonance Raman spectroscopy is that it has effectively no time-resolution in the sense that the experimenter cannot control the time after excitation as to when the sample is probed. Effectively everything occurs within the laser pulse and thus the dynamics of the system determine which species is measured. In conventional MLCT systems in which there is only one state, the ^{3}MLCT, this is not such a serious restriction, but in systems with more than one chromophore and thus a number of excited states this is a fundamental weakness of this type of experiment.

These two restrictions are readily solved by using a two-colour time-resolved resonance Raman experiment (TR^3). In this one of the pulses acts as a pump and is coincident with the ground state absorption and the second colour pulse is coincident with the excited state absorption and delay between the two may be controlled to derive a true time-resolved experiment.[103, 104]

4 Case studies

4.1 Conventional MLCT systems

Conventional MLCT systems are those in which each ligand contributes to one low energy transition and there are not a myriad of close-lying excited states on each ligand. These systems have been extensively studied over the past few decades. Complexity in function and photophysics can be built into these systems by the use of differing ligands, such as in chromophore-quencher complexes[105-107] or heteroleptic complexes.[108-116] In addition even the apparently simplest MLCT systems may be affected by ancillary ligands that can play a significant role in the photophysics and spectroscopic properties. An example of this is the nature of X in the M-X system (M = metal, X = halide), which can influence the type of transition that is observed.[117-120] Although the direction of electron density change is similar, it has been found that when X is larger, the excited state character that predominates is XLCT rather than MLCT, which can be attributed to increased halide character in the HOMO of the complexes. Some of the first studies to investigate this were done on $[Ru(X)(R)(CO)_2(N\text{^}N)]^+$, where R = alkyl and X was varied between Cl^-, Br^-, and I^- using a combination of spectroscopic techniques. For R = CH_3 and N^N = *i*Pr-DAB (N,N'-diisopropyl-1,4-diaza-1,3-butadiene) the excited state $\tilde{\nu}$(CO) modes were found to shift to higher energies in the TRIR spectra, consistent with MLCT excitation. However, the magnitude of this shift decreased in the order $Cl^- > Br^- > I^-$, which indicates an increased amount of electron density on the Re metal in the excited states. CO bond length changes were approximated to be 0.009

Å for the Cl^- and Br^- complexes and 0.006 Å for the I^- complex. Excited-state Raman experiments showed a similarly systematic decrease of the $\tilde{\nu}$(CN) of the *i*Pr-DAB ligand, indicating an increase in electron-density on the ligand. This was interpreted as a change in excited state character toward XLCT for heavier X. A similar result was obtained for $[Re(CO)_3X(bpy)]^+$. For these complexes, the XLCT states are longer-lived and have higher emission quantum yields compared to their MLCT counterparts.

4.1.1 $[Re(CO)_3(L)(N^N)]$ complexes

Complexes of the form $[Re(CO)_3(L)(N^N)]^+$ are particularly amenable to study using vibrational spectroscopy due to the diagnostic nature of the carbonyl modes, which possess bands in isolated spectral regions. As a result TRIR has been extensively used to investigate these systems. With some exceptions TRIR has revealed that for L = Cl^- the prevalent excited state observed is of MLCT nature.[41, 44, 82, 102, 121-125] Recently an additional minor state consisting of MLCT and IL components has also been described[126] for compounds where L = Cl^- and imH (imidazole) and NN = dmp, phen and bpy. This additional state is visible as a red shoulder of the a'(1) mode at early times after photoexcitation and its assignment has been carried out with evidence from transient absorption measurements and detailed DFT calculations. It has been suggested that similar states exist for many additional compounds but may be overlooked due to their low intensity and short-lived nature.

There are some cases for which L = Cl^- and where photoexcitation leads the formation of states other than MLCT, which are discussed here. A relatively straightforward example is $[Re(CO)_3Cl(5\text{-}NO_2\text{-}phen)]$. As would be expected from similar complexes, photoexcitation in MeCN produces a ^{1}MLCT state that undergoes ISC to a ^{3}MLCT state on a sub-ps timescale, leading to a shift of the $\tilde{\nu}$(CO) bands to higher energy in the TRIR spectra. These $\tilde{\nu}$(CO)

bands are rapidly (ca. 10 ps) replaced by a new set, shifted to lower energy with respect to the parent. This behaviour was assigned to the formation of a IL(n,π*) state, which decays to the ground state in 30 ps.

Complexes with pyridyl-1,2,3-triazole (Pytri-R) ligands (Figure 5) are of interest for two reasons: firstly the use of "click" chemistry in their synthesis means that there is considerable scope for substitution on the ligand, and secondly, the compounds show that the triazole ring acts as an electronic insulator and substituents have little effect on the spectral properties. In a systematic study of $[Re(CO)_3Cl(Pytri\text{-}R)]$ complexes Kim et al.[127] showed that the resonance Raman spectra of the complexes appeared almost identical with substituents linked by a methylene group. Additionally it was found that the excited and electrochemical properties were also similar. These findings were supported by DFT calculations that revealed the lowest excited state to be MLCT in nature with virtually no contribution from the substituent unit.[128] This lack of communication has been utilised advantageously to create supramolecules in which luminophores are not quenched when the supramolecule forms through binding with a heavy metal (in this case palladium). [129, 130]

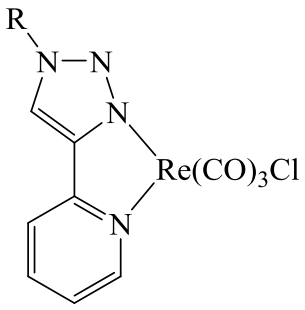

R =
C_8H_{17}
CH_2Ph
CH_2PhOMe
CH_2PhNO_2
Ph
Fc
PhOMe
$PhNO_2$

Figure 5. Structure of Pytri-R complexes and their substituents incorporated using "click" chemistry. [127, 128]

The use of larger N^N ligands with multiple compartmentalised sections or appended donors is interesting as they can play more active roles in the photophysics of their complexes; as

discussed in some detail in this review, one of these ligands is dppz. The excited states of [$Re(CO)_3Cl(dppz\text{-}X_2)$] complexes have been shown to be predominantly of MLCT character but for X = H and Me, a significant LC component was observed as well.[44] More recently, we have examined a dppz complex substituted by more strongly electron-donating groups, which produced dominant LC states (*vide infra*).

Deviation from the typical MLCT-forming behaviour is also observed for the dmpy class of ligands (dmpy = 3-R-1-(2-pyridyl)-imidazo[1,5-α]pyridine, see Figure 6). Several electron-rich and electron-poor R groups have been investigated.[131] Two new bands shifted to lower energy with respect to the parent a'(1) mode can be identified in TRIR, indicated as HE1 and HE2 in Figure 6, whereby HE1 converts to HE2 in tens of picoseconds. This is attributed to a slow ISC from ligand-centred S_1 to T_1 states. The slow nature of the ISC was explained by symmetry-constraints in the spin-orbit coupling, which essentially isolates the metal subunit from the ligand. Significant charge-transfer character was observed for the S_1 states of compounds with the relatively electron-donating Ph-NMe_2 substituents, which manifested in an increased shift in the $\tilde{\nu}$(CO) vibrations compared to T_1. Interestingly charge transfer was observed for S_1 states of compounds with both electron-withdrawing and electron donating substituents, where the nature of the substituent determines the direction of charge transfer.

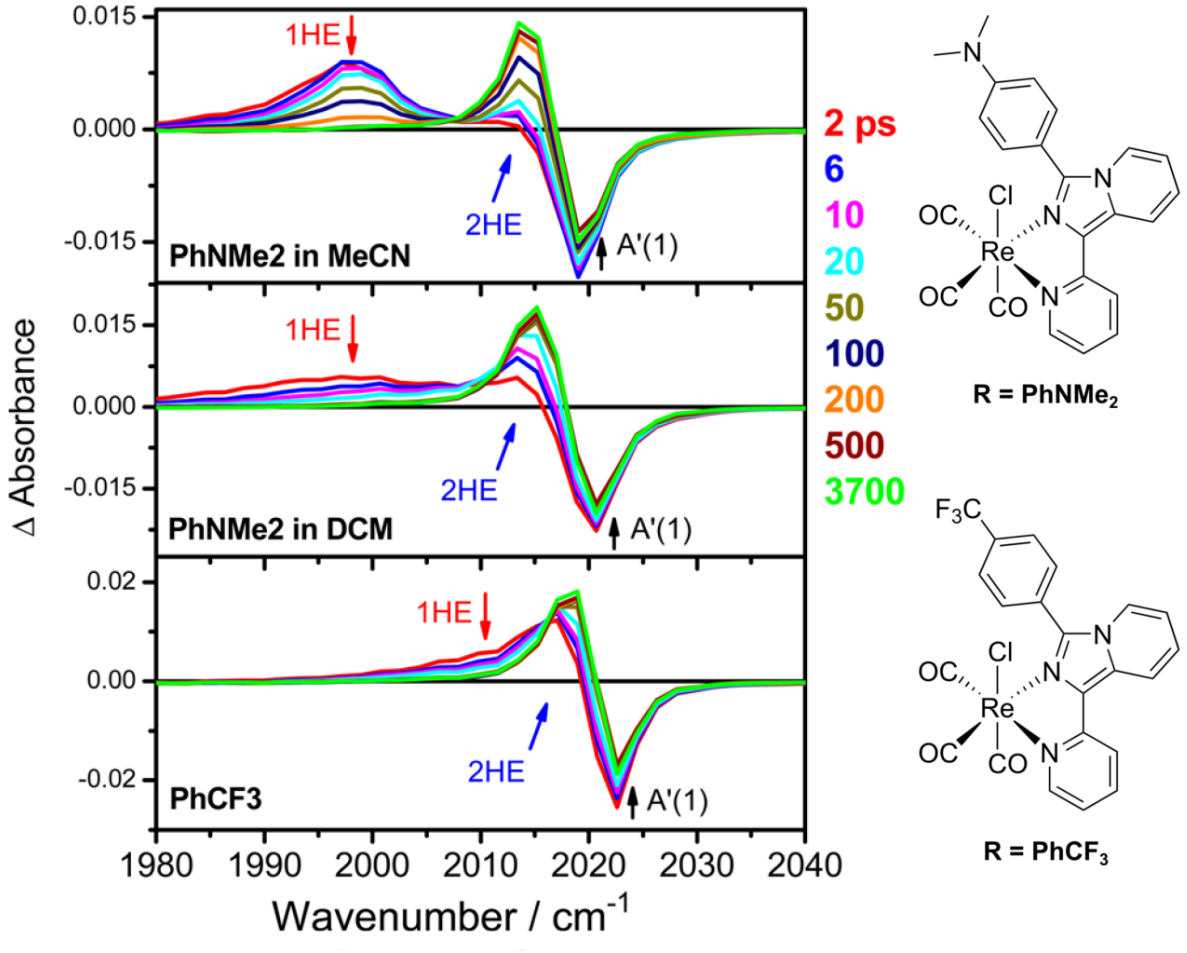

Figure 6. ps-TRIR spectra of [Re(CO)3Cl(R-dmpy)] after 400 nm photoexcitation, indicating HE1 and HE2 features. Shown are R = PhNMe2 in MeCN (top) and in dichloromethane (middle), and R = PhCF3 in dichloromethane (bottom). Adapted with permission from ref. [131] Copyright (2008) American Chemical Society.

Finally, there are a number of multi-component systems based on $[Re(CO)_3Cl(N^N)]^+$ that are designed to facilitate movement of charge in the excited state and effect the formation of different excited states.[132, 133] Movsisyan et al.[133] examined the interplay between a rotaxane with a phen-based macrocycle containing the $\{Re(CO)_3Cl\}$ fragment (abbreviated **M(Re)**) and a hexayne-based chain (abbreviated **H**). The structures and photophysical processes of the rotaxane are summarised in Figure 7. Photoexcitation of only **M(Re)** leads to

a mixed IL/MLCT state that quickly converts to pure MLCT, until it returns to the ground state (τ = 93 ns). In the case of the rotaxane (**H⊂M(Re)**), selective excitation of the rhenium chromophore (λ_{ex} = 350 nm) again leads to the formation of similar initial states; however, after formation of the MLCT state energy transfer occurs to the a triplet excited state of the hexayne component in *ca.* 1.5 ns. This hexayne-localised state in the **H⊂M(Re)** system has a lifetime of 20 µs; it is the same state as obtained upon selective excitation of the chain (λ_{ex} = 310 nm) and indeed very similar to that observed when only **H** is present.

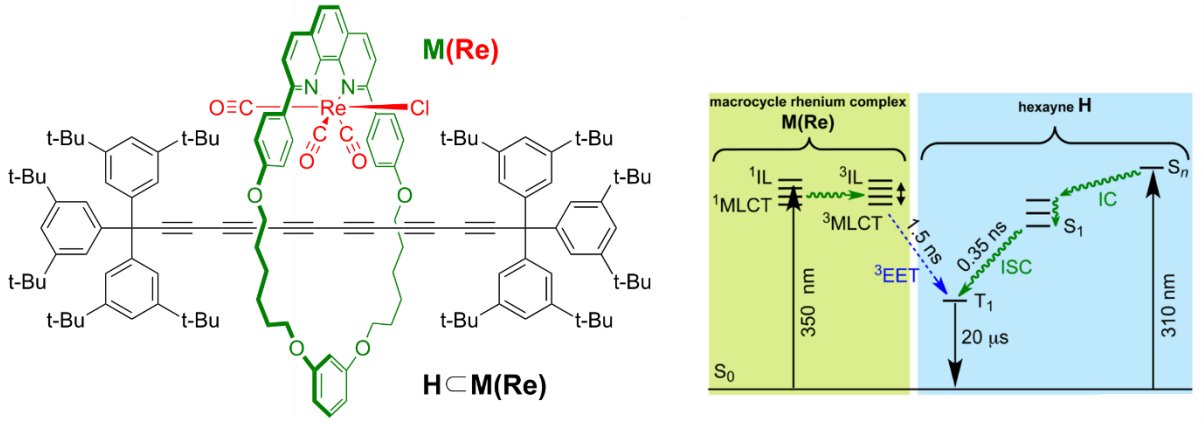

Figure 7. Structure of **H⊂M(Re)**, consisting of the hexayne chain **H** and rhenium-based macrocycle, **M(Re)**. A summary of the photophysical processes of **H⊂M(Re)** is shown on the right. Adapted with permission from ref. [133] Copyright (2014) American Chemical Society.

Imidazoles have also been used as L substituents in the $[Re(CO)_3(L)(N\text{^}N)]^+$ system.[134] [135] When N^N = phen, relatively straightforward photophysical properties were exhibited, with TRIR identifying the lowest excited state as MLCT in nature, while substitution of phen by NO_2 caused subsequent formation of a LLCT state that decayed rapidly to the ground state or decomposed. However, imidazole has also been employed as a linker of $\{Re(CO)_3(LL)\}^+$ (LL = phen or dmp, 2,9-dimethyl-1,10-phenanthroline) to *Pseudomonas aeruginosa* azurins

to act as a reporter label to probe for picosecond to microsecond changes of electron density.[134, 136-138] These rhenium fragments were not found to perturb peptide folding. When linked to the 124-position, photoexcitation of the rhenium centre initially produced a MLCT state, which rapidly charge-separated to oxidise the azurin Cu(I) via several spectroscopically characterised intermediates.[136] The electron-transfer proceeded two orders of magnitude faster than would be expected for a single-step tunnelling process, indicating that multi-step tunnelling is involved, identified as proceeding through a tryptophan residue at position 122 of azurin. Substitution at a number of additional positions of azurin have allowed probing of electron-injection dynamics across the protein.[137]

As discussed above, changing the N^N ligand of $[Re(CO)_3(L)(N^N)]^+$ perturbs the photophysics of the resulting complexes, although all considered ligands remain nitrogen donors. Altering L often results in more significant effects, due to the influence of the ligand's back-bonding ability on the metal dπ orbital energies. While the initially populated states for L = Cl^- and L = py (and derivatives) can be similar, changes may manifest in the lowest-energy excited states. In the case of L = NCS, mixing of excited states occurs. The NCS^- unit in $[Re(CO)_3(NCS)(N^N)]$ (N^N = bpy, ^{i}Pr-DAB) acts as an additional reporter group for vibrational spectroscopic investigations. [139]. Resonance Raman carried out at 400 nm, overlapping with the lowest-energy absorption band, indicates bond-length changes in the C≡O and N=C=S groups, which is evidence for both MLCT and ligand-to-ligand charge-transfer (LLCT) transitions. Upon photoexcitation, TRIR spectra showed a shift of ν(CO) to higher energies and of ν(CN) to lower energies; the opposing signs of shifts are due to removal of electron density from the π* antibonding and π bonding orbitals of the C≡O and N=C=S groups respectively. With the additional aid of DFT calculations, the lowest-

energy excited states were assigned as {$Re(CO)_3(NCS)$} → N^N, consisting of mixed MLCT and LLCT character.

The attachment of nitrogen-donor ligands affords possibility for substitution larger, more conjugated groups as well as electron-donating and electron-accepting[106, 107, 140-142] moieties. For L = stpy[142] or bpe[140] (*t*-stpy = *trans*-4-sterylpyridine, bpe = 1,2-bis(4-pyridyl)ethylene where NN = bpy or phen), stilbene-like isomerization was investigated using time-resolved Raman and IR techniques. For L = *t*-stpy, initial formation of a ^{3}MLCT(bpy) state occurs, which converts rapidly (3.5 ps) to a stpy-localised ^{3}IL state; this rotates by 90° around the C=C bond (12 ps), forming the perpendicular or *p*-stpy geometry from where isomierization to *cis*-stpy is possible. In contrast to this, the photoisomerisation of *t*-stilbene occurs in the singlet state.

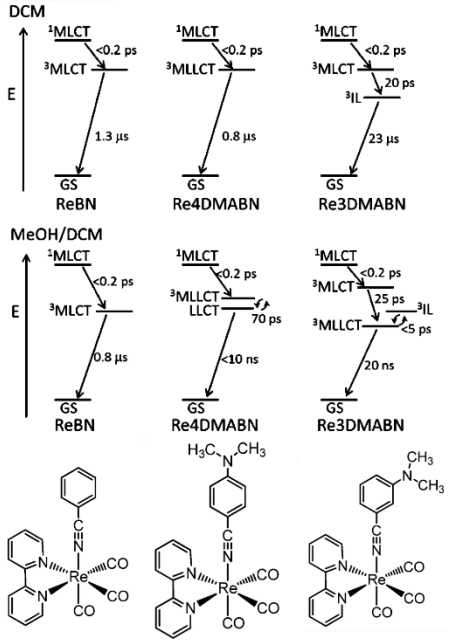

Figure 8. The photophysical processes of $[Re(CO)_3(L)(bpy)]^+$, where L = BN, 4-DMABN and 3-DMABN after photoexcitation at 402 nm. Used with permission from ref. [80]. Copyright (2013) American Chemical Society.

More recently, a series of L = BN (benzonitrile) substituents have been investigated using TRIR, where NN = bpy and L = BN, 4-DMABN (4-dimethylaminobenzonitrile), and 3-DMABN (3-demethylaminobenzonitrile).[80] The photophysics of these complexes, which are summarized in Figure 8, were found to be rather sensitive to the substitution pattern on the BN and solvent, due to the presence of several close-lying states. A change in solvent polarity modulates the energies of the charge-transfer transitions, making them favoured in the dichloromethane:MeOH solvent system. The effect of the substitution pattern is explained by the presence of quinoidal resonance structures for 4-DMABN, which allow for charge-transfer to be coupled across the entire ligand (*cf.* 3-DMABN, where the charge would originate mostly from the amine). This strongly couples the MLCT and CT states and thus the LLCT state indicated in Figure *8* is only of partial CT character. These findings were later used to further modulate the energy of the acceptor orbital (by using dicarboxyethyl-bpy), effecting the transfer of effectively a full electron in the excited state for the 3-DMABN complex.[143]

4.2 MLCT, LC π,π systems*

In dppz complexes it is not possible to simplify the electronic structure – the ligands are imbued with a number of close-lying orbitals that inevitably form chromophores with metals that are MLCT and LC π,π* in character. The intrinsic complexity of these systems and the ambiguity of excited state nature has made these systems well-suited to examination by time-resolved vibrational spectroscopy and resonance Raman spectroscopy to examine the Franck-Condon state.

For dppz complexes, the first excited state identified using time-resolved vibrational spectroscopy was of $\pi \rightarrow \pi^*$ character, which was found to be the lowest energy excited state

of $[Re(CO)_3(PPh_3)(dppz)]^+$.[76] As this state does not couple to any other, it has a rather long lifetime of 42 μs at room temperature. Many of the subsequently investigated complexes are shorter-lived, which can be attributed to coupling with deactivating excited states.

Resonance Raman spectroscopy, which is a complementary technique to infrared, has been extensively used in studies on dppz complexes. Its advantages include that it allows the initially formed excited Frank-Condon (FC) state to be probed and that aqueous solutions are more easily studied (although some TRIR studies have been carried out in D_2O[43, 45, 144]), making the study of biological systems more accessible. A drawback is that the intensity of CO reporter ligands is much smaller and depends on the probe wavelength, making Raman techniques less diagnostic as far as the assignment of excited states is concerned. They are for this reason often applied in conjunction with computational techniques, which can be useful in the interpretation of results. A generic challenge in studying dppz systems is that the vibrational spectra from the dppz and ancillary ligands are similar and the result is a congested spectrum of overlapping bands.[47]

It is possible to use resonance Raman spectroscopy in a more nuanced way to understand the types of acceptor orbitals in transition involving dppz. In the simplest complexes, such as $[Re(CO)_3Cl(dppz)]$ or $[Cu(PPh_3)_2(dppz)]^+$, in which the ancillary ligands are not chromophore active in the visible region and the activity is from dppz only, the main low energy chromophore is the MLCT(phen) transition. This often appears as a shoulder on the red edge ($\lambda > 420$ nm) of the $\pi \rightarrow \pi^*$ ligand-centered transition ($\lambda \sim 380$ nm).[145] The MLCT(phz) has no oscillator strength because of the paucity of overlap between the metal $d\pi$ MOs and the phz π^* MO. The resonance Raman spectra are consistent with this as they show the enhancement of vibrational modes that are phen in nature. The spectral features are exemplified by the resonance Raman spectrum ($\lambda_{ex.}$=457.9 nm) for $[Re(CO)_3Cl(dppz)]$; this shows bands at 1316, 1350, 1450, 1575 and 1597 cm^{-1} that are all phen-modes. The

additional bands at 1406 and 1545 cm^{-1} are phz-based or delocalized across the ligand framework. The assignment of these modes is supported by a number of DFT and ligand deuteration studies.[57, 145-148] The changes in enhancement patterns with λ_{ex} show stronger enhancement for phz modes as $\lambda_{ex.}$ is tuned to blue wavelengths where resonance with the $\pi \rightarrow \pi^*$ ligand-centered transitions occur.

A number of strategies have been employed to try to obtain unambiguous resonance Raman spectral signatures for the differing excited states present in dppz complexes. Waterland et al.[145, 149] used spectroelectrochemistry to observe the spectrum of reduced $[Re(CO)_3Cl(dppz^{-})]$ and $[Cu(PPh_3)_2(dppz^{-})]^+$ species to isolate $dppz^{-}$. Strong features at 1581 and 1368 cm^{-1} were observed. (The 1581 cm^{-1} band is actually a phen mode of the $dppz^{-}$; this assignment was made based on DFT calculations and deuteration studies.[146]) A variety of dppz ligands with substitution at the 11 and 12 positions (Figure *1*) were used in the study including NO_2, CH_3 and Cl. The spectroelectrochemical data were compared with single-colour TR^2 measurements on the complexes. Assignments could then be made based on whether the $dppz^{-}$ bands were evident. Of the systems studied $[Re(CO)_3Cl(dppzNO_2)]$ showed he clearest evidence for an MLCT excited state with the other complexes being predominantly π,π in nature.[145] The TR^2 spectra of the free ligand have also been measured and compared with the spectra of the complex as representative of the $\pi \rightarrow \pi^*$ state.[26, 150] These assignments were later corroborated and expanded upon by TRIR studies[42, 47] illustrating the complementarity of these two techniques.

4.2.1 Considerations when interpreting time resolved resonance Raman spectra

Resonance enhancement can skew identification of particular states; if multiple states are present and one possesses a much greater absorption then it will dominate in the Raman

spectrum – for example, the radical anion of dppz has shown significant differences in enhancement patterns when probed at 350 and 396 nm.[151] Thus the lack of an observed excited state does not rule out its presence. The use of transient absorption as well as several Raman probe wavelengths can therefore be important.

The presence of MLCT(phen), MLCT(phz) and more than one type of $\pi \rightarrow \pi^*$ state has been shown as the lowest occupied state for substituted complexes of the form $[Re(CO)_3L(dppz)]$ (L = halogen or pyridine-based ligand). Changing L, the substituents and substitution pattern on dppz (most commonly at the 11,12-positions, see Figure *2*) affords control over the states accessed after photoexcitation and thus can be used to tailor a complex toward a particular application.

It has been established [152, 153] using temperature-dependent fluorescence studies that for $[Ru(phen)_2(dppz)]^{2+}$ entropic factors favor the higher-energy MLCT(phen) state over the lowest-energy phz-based state. Reducing the enthalpy gap between these states can contribute to the preferential population of MLCT(phen), which is desirable from the perspective of photophysical probes, as this state shows bright luminescence. While the entropic preference of MLCT(phen) has been shown to be true for a number of complexes,[44] other factors such as the ancillary ligands can also play a role (see below). Here we show a number of ways in which the modification of rhenium dppz-based complexes can result in a change in the ordering of the excited states and thus the excited-state properties of the complexes.

Substituted $[Re(CO)(L)(dppz)]^+$ is convenient for the characterisation of dppz-based excited states as the excited-state electron is usually located on the dppz ligand. This section will therefore mainly focus on the modification of this motif, with some reference made to other complexes. The ancillary ligand L plays a role in determining the excited state formed but, with some exceptions,[141] does not itself act as an electron donor or acceptor. For example, it has been found that the population of the $\pi \rightarrow \pi^*$ over MLCT states can be

modulated by changing L from Cl^- to py (py = pyridine).[125] This can be explained by the relative electron-withdrawing nature of py-based ligands compared to Cl^- which is expected to lower the energy of the dπ orbital, thus increasing the energy of the MLCT states and leading to preferential population of the $\pi \rightarrow \pi^*$ state (see Figure 9(a)). Therefore, $\pi \rightarrow \pi^*$ states are often present where L is not a strong electron donor. In comparison to MLCT excited states the lifetime of the $\pi \rightarrow \pi^*$ state can be much longer[76, 154] and is dependent to a large extent on the communication with the MLCT states, through which rapid deactivation can proceed.

Similarly, the ancillary ligands of heteroleptic ruthenium complexes can affect the excited states formed.[38] For example, comparing the excited-state lifetime of $[Ru(phen)_2(dppz)]^{2+}$ (which possesses a pure MLCT state) to that of $[Ru(en)_2(dppz)]^{2+}$ (en = ethylenediamine) indicates that the latter possesses an excited state configuration that can be described as dppz-centered $\pi \rightarrow \pi^*$ in equilibrium with MLCT.[155] The complex $[Ru(tmBiBzIm)(dppz)(tbbpy)]^{2+}$ (tmBiBzIm = 5,5',6,6'-tetramethyl-2,2'-bibenzimidazole, tbbpy = 4,4'-di-tert-butyl-2,2'-bipyridine) includes the pH-responsive tmBiBzIm ligand; upon deprotonation the excited state lifetime is reduced by a factor of 50 in CH_3CN and the lowest-energy electronic absorption band red-shifts by *ca.* 3400 cm^{-1}. While it might be concluded that this indicates active involvement of the tmBiBzIm ligand, using resonance Raman it was shown that the fundamental nature of the electronic transitions remained the same upon deprotonation and, in fact, excitation of the low-energy absorption band involves solely the tbbpy and dppz ligands.[156]

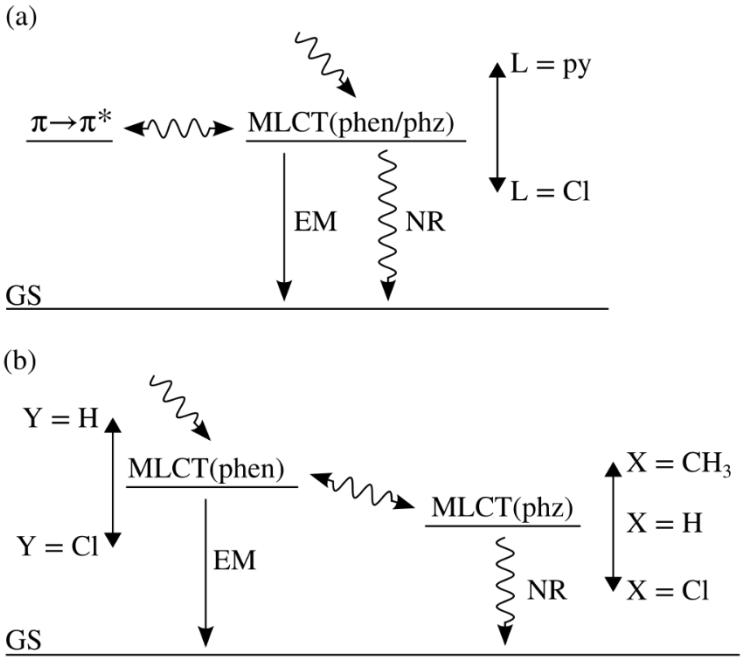

Figure 9. (a) Modification of the ancillary ligand L of $[Re(CO)_3L(dppz)]$ changes the energy and population of the MLCT states. (b) Modification of the substituents on the phenazine (X) and phenanthroline (Y) moieties changes the energy of the MLCT(phz) and MLCT(phen).[41, 44, 157]

Substitution of dppz has been carried out on several positions of the ligand;[41, 44, 157] generally modification of the phenazine and phenanthroline portions of the ligand affects the energy of the associated molecular orbital. Substituents on the 11,12-positions and 2,7-positions will be referred to as X and Y respectively (see Figure 2). Altering the X substituent of $[Re(CO)_3Cl(Y_2\text{-dppz-}X_2)]$ clearly changes the occupancy of the lowest excited state. Using TRIR it was shown that for X = CH_3 and X = H in CH_2Cl_2 a mixture of $\pi \rightarrow \pi^*$ and MLCT(phen) states is formed, with a greater contribution of the $\pi \rightarrow \pi^*$ state for the more electron-donating CH_3 substituents; for X = Cl the predominant state is MLCT(phz). As shown in Figure 9(b), this behavior can be explained by the stabilizing effect of the substituents on the MLCT(phz) state and thus the relative population in the excited state.

These results correlate well with emission studies, which show MLCT(phen) emission from the complexes substituted with CH_3 and H. As MLCT(phz) states tend to undergo fast non-radiative decay to the ground state, the compound with X = Cl is non-emissive, even in apolar solvents. It would similarly be expected that changing Y leads to a change in the MLCT(phen) energy, as indicated in Figure 9 (b). This has been shown to be true for $[Ru(L1)_2(Y_2\text{-dppz-}X_2)]^{2+}$ (L1 = bpy, 4,4'-*tert*-butyl-bpy), which have been studied using resonance Raman and luminescence spectroscopy. A prolonged excited-state lifetime was found when Y = Br, compared to Y = H; [148, 158] conversely, for X = Br, both the excited state lifetime and luminescence quantum yield decreased. In both cases this can be attributed to preferential population of the substituted portion of the ligand.

A number of different substitution patterns and additional metals have been explored aside from those discussed here,[159] [38, 148, 158, 160] and these can be used to further fine-tune the excited states formed and their lifetimes.

4.2.2 Biological applications and medium effects

A number of biological applications have been developed for complexes of dppz[38, 160, 161] and indeed, many initial TR^3 studies focused on the interactions of $[Ru(N\text{^}N)_2(dppz)]^{2+}$ (N^N = bpy or phen) with DNA.[88, 151, 162, 163] This has been discussed in more detail previously.[47] While the photo-oxidation of DNA by ruthenium dppz complexes often proceeds via reactive oxygen intermediates,[160] complexes of rhenium have been shown to be able to directly photo-oxidize guanine while bound to DNA.[45, 46] TRIR has been used to monitor this, using $[Re(CO)_3(dppz)(py\text{-}R)]^+$ (R is propanoic acid or propanoate ester).[46] As well as MLCT(phen) states, two $\pi \rightarrow \pi^*$ excited states were observed, assigned as phen-based and phz-based. By monitoring both the $\tilde{\nu}$(CO) and ν(DNA) regions of the IR spectrum

it was established that hole-transfer, from the excited complex to guanine can occur directly from the MLCT(phen) or $\pi \rightarrow \pi^*$(phen) state, while the $\pi \rightarrow \pi^*$(phz) state appeared to be inactive. A challenge with these measurements is the similarity of the $\tilde{\nu}$(CO) bands of the $\pi \rightarrow \pi^*$(phz) state of the excited complex to the reduction product as both species feature an electron in the π^*(phz) orbital of the dppz ligand. However, these species are expected to show significant differences in resonance Raman enhancement and should therefore be accessible for identification using TR^3 spectroscopy.

Alternatively TRIR spectra in the spectra in the ligand (and DNA) stretching regions can be used to gain more structural insight and allows the use of complexes without reporter ligands; this has been done recently with the $[Ru(TAP)_2(dppz)]^{2+}$ (TAP = 1,4,5,8-tetraazaphenanthrene).[164, 165] In order to precisely determine the location of the ruthenium complex within the DNA, TRIR was carried out on crystals of a decamer sequence of nucleic acids containing Λ-$[Ru(TAP)_2(dppz)]^{2+}$, which allowed for x-ray crystallography to be carried out on the same sample. A primary site for electron transfer was identified as a guanine in the intercalation cavity, indicating that spatial proximity to guanine is the major factor determining the electron transfer. Dynamics were found to be similar to solution-phase studies, which suggests that structural flexibilities present in solution play less of a role in the electron-transfer.

A further example of TRIR spectroscopy without the presence of reporter ligands is the complex $[Cr(phen)_2(dppz)]^{3+}$.[166] It was found that the presence of guanine-containing DNA significantly decreases the lifetime of the complex (to 3 ps compared to > 50 μs in the absence of DNA). A bleaching pattern resembling direct excitation of DNA was observed; however, bands corresponding to 1-electron oxidized guanine could not be confirmed, indicating extremely efficient electron back-transfer for this complex.

4.3 Engineering new chromophores on ligands

One of the earliest reports on the substitution of polypyridyl ligands with independent chromophores was by Tyson et al.[167, 168] in which it was shown that the incorporation of coumarin-based dyes into ruthenium complexes (Figure 10) could deliver long-lived excited states and large oscillator strengths.[169-171] This was further developed using perylene and naphthalimide groups.[172-176] In the case of the naphthalimide substituents both MLCT and LC π,π* states were evident. The evidence for the LC π,π* state was elegantly demonstrated using time-resolved infrared spectroscopy in the 1400 – 1800 cm^{-1} region which showed that the transient created in $[Ru(phen)_2(PNI)]^{2+}$ was identical to that from tolyl-PNI (Figure 10).[177] In both cases the infrared bands from the imide carbonyl groups inform on the excited state. For tolyl-PNI the ground state bands at 1705 and 1657 cm^{-1} downshift to 1636 and 1598 cm^{-1}, for $[Ru(phen)_2(PNI)]^{2+}$ the carbonyl band frequencies shift from 1705 and 1668 cm^{-1} to 1643 and 1597 cm^{-1}. The use of the same PNI group of $[Re(CO)_3Cl(PNI)]$ produced a long-lived ^{3}LC excited state (τ = 650 μs); by using TRIR it was possible to observe the evolution of the FC state (a ^{1}LC state) to ^{3}MLCT over 45 ps and then to ^{3}LC in 15 ns. This so-called ping-pong mechanism has the energy jumping from one chromophore to the next and back with a change of spin in the process. The strong and distinctive spectral features associated with the $\{Re(CO)_3\}$ fragment combined with the mid-IR signatures from PNI made this possible (Figure 11).[178] In this case the downshift of the imide carbonyls (from 1714 and 1673 cm^{-1} to 1660 and 1610 cm^{-1}) indicates the ^{3}LC PNI-based state and the upshift in the metal carbonyl frequencies (from 2019, 1918 and 1893 cm^{-1} to 2055 and a broad feature at 1970 cm^{-1}) is indicative of the MLCT state.

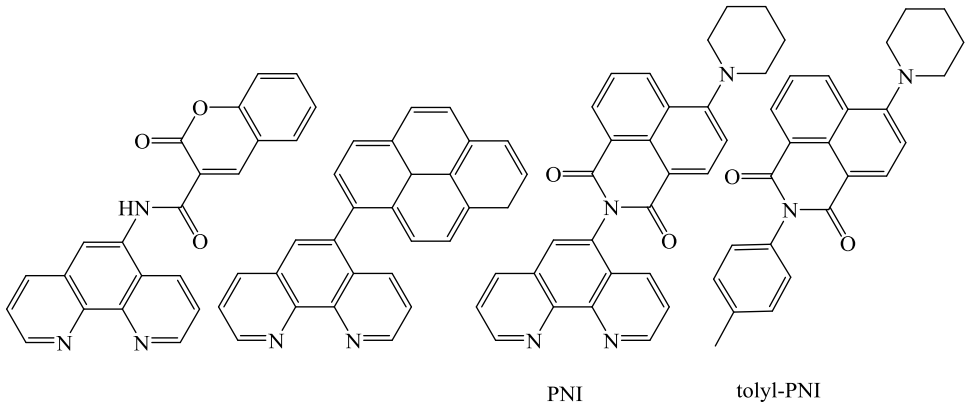

Figure 10. Ligands used to create long-lived excited states in Ru and Re complexes and the model system tolyl-PNI. [167, 172, 173, 177, 178]

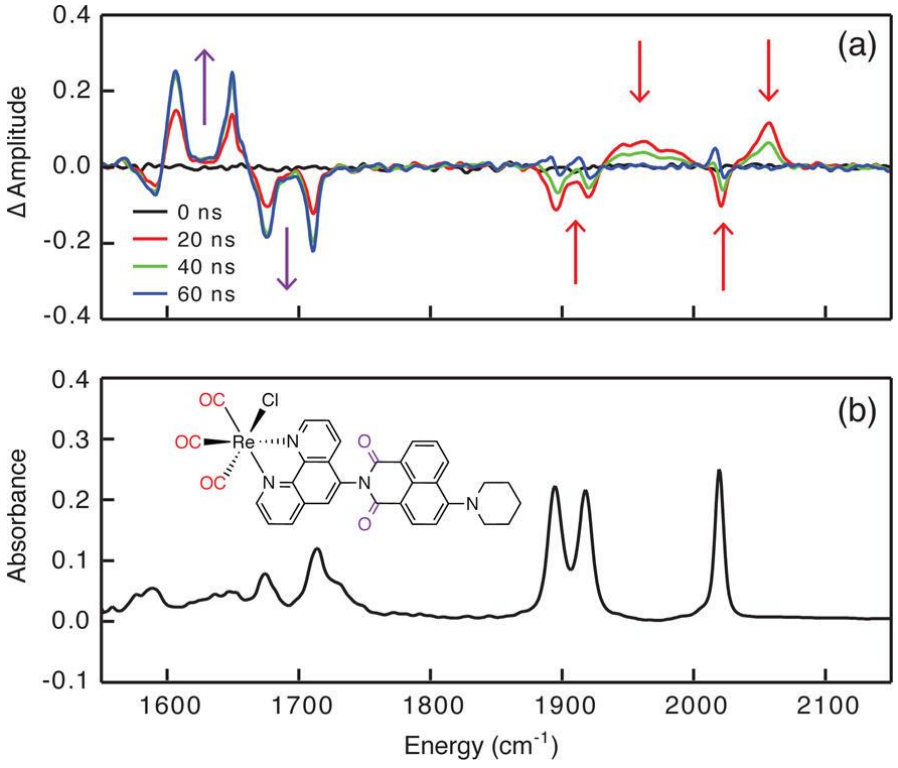

Figure 11. Ground-state FTIR spectrum (b) and time-resolved step-scan (a) FTIR difference spectra of $[Re(CO)_3Cl(PNI)]$ in THF following 410 nm pulsed excitation (5 - 7 ns fwhm). Reprinted with permission from ref. [178]. Copyright (2011) American Chemical Society.

The increase in absorption from the dyes discussed above was derived from adding chromophores however it is also possible to create new chromophore systems using donor groups. One example of this a study of sulfur substituents on dppz.[179] The presence of donating sulfur containing species (thioether and thiocarbamate at the 11, 12 positions, Figure *1*) on the dppz ligand formed strongly coloured rhenium(I) complexes with intense absorption (ε ~ 40,000 $M^{-1}cm^{-1}$) at 450 nm. These transitions were probed using resonance Raman spectroscopy and analysis of the band enhancement pattern in concert with DFT calculations pointed to a transition that had significant ILCT character. The effect of donor groups on dppz was further explored in a study of 11-(4-diphenylaminophenyl)dppz (dppz-$PhNPh_2$) complexes of the type $[Re(CO)_3R(dppz\text{-}PhNPh_2)]^+$, where R = Cl^-, py, 4-dimethylaminopyridine (dmap).[51] Complexes with this ligand showed intense absorption in the visible region (ε ~ 20,000 $M^{-1}cm^{-1}$). The shifts in these bands was not consistent with an MLCT transition as the substitution at the ancillary ligand with R = py and dmap show bands at 520 nm and with R = Cl^- at 452 nm. Resonance Raman spectroscopy reveals the presence of a single dominant transition across the entire visible spectrum which showed no enhancement of CO bands. In fact the resonance Raman spectra barely altered across the absorption band supporting the assignment of a single dominant electronic transition. DFT calculations suggested this was an ILCT transition. Using TRIR it was possible to confirm this assignment. Detailed analysis of the TRIR of the complex $[Re(CO)_3(dmap)(dppz\text{-}PhNPh_2)]^+$ (dmap = 4-dimethylaminopyridine, dppz-$PhNPh_2$ = 11-(4-diphenylaminophenyl)dppz) displays up to three potential features in the excited state IR spectrum that appear to lower energy than their parent depletions, indicating the presence of several $\pi \rightarrow \pi^*$ states.[51] As these features are spectrally close and subtle shifts (*ca.* 3 cm^{-1}) occur on the ps timescale, use of the carbonyl region was not sufficient to definitively identify their presence or define processes as vibrational cooling or excited-state

interconversion. By carrying out ps-TRIR in the ligand-stretching region (see Figure *12*) spectral differences between the states were made evident.

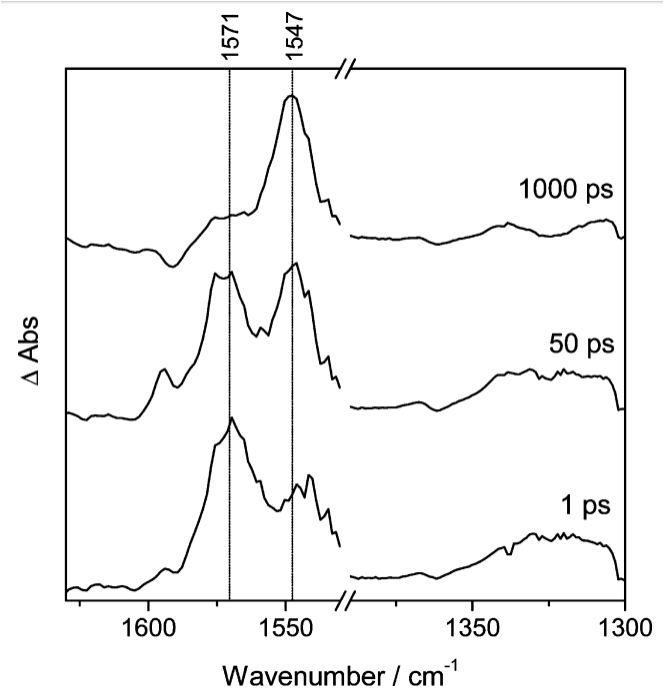

Figure 12. TRIR spectra of the complex $[Re(CO)_3(dmap)(dppz\text{-}PhNPh_2)]$ at a number of time-delays after photo excitation at 400 nm. Reprinted with permission from ref. [51]. Copyright (2014) American Chemical Society.

The use of donor groups may also be used in binuclear and larger multi-metal systems (Figure 13). The ligand HATN can form mono- bi- and tri-nuclear complexes with $\{Re(CO)_3Cl\}$. A number of isomers are possible and these may be synthesised using different solvent systems.[82] These complexes show strong visible absorption that are MLCT in nature, red-shifted from 530 to 650 nm on going from mono- to tri-nuclear complex. This assignment was confirmed by resonance Raman spectroscopy in which carbonyl bands were enhanced. TRIR studies showed band shifts in the CO region associated

with an oxidised rhenium centre and two spectator ligands bound to a reduced HATN moiety. For the complex $(Re(CO)_3Cl)_3(\mu\text{-}HATNMe_6)$ the highest frequency CO band (the symmetric stretch) shows an upshift for the oxidised Re from 2024 to 2073 cm^{-1} with a downshift from 2024 to 2014 cm^{-1} associated with the two unoxidised Re centres now bonded to a $HATN^{\cdot-}$ radical anion.

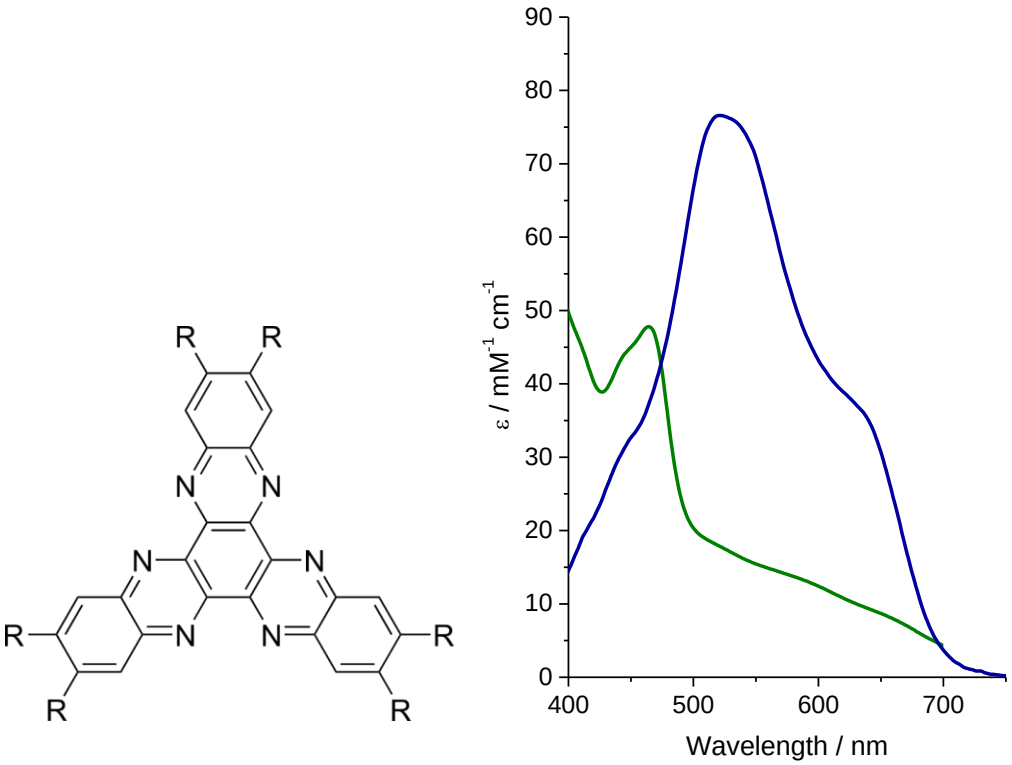

Figure 13. Structure of the HATN ligand (left), where R = CH_3 ($HATNMe_6$) or SC_8H_{17} ($HATN(SC_8H_{17})_6$). Electronic absorption spectra (right) for $(Re(CO)_3Cl)_3(\mu\text{-}HATNMe_6)$, green trace and $(Re(CO)_3Cl)_3(\mu\text{-}HATN(SC_8H_{17})_6)$, purple trace, in CH_2Cl_2. [82, 180]

By using SC_8H_{17} groups on the periphery of the HATN ligand it was possible to make a series of rhenium complexes with very high absorption (ε ~100000 $m^{-1}cm^{-1}$) compared to the parent species.[51] The FC states across these intense absorption bands were probed with resonance Raman spectra and revealed the presence of a number of states. Using $(Re(CO)_3Cl)_3(\mu\text{-}HATN(SC_8H_{17})_6)$ as an example (Figure 14)

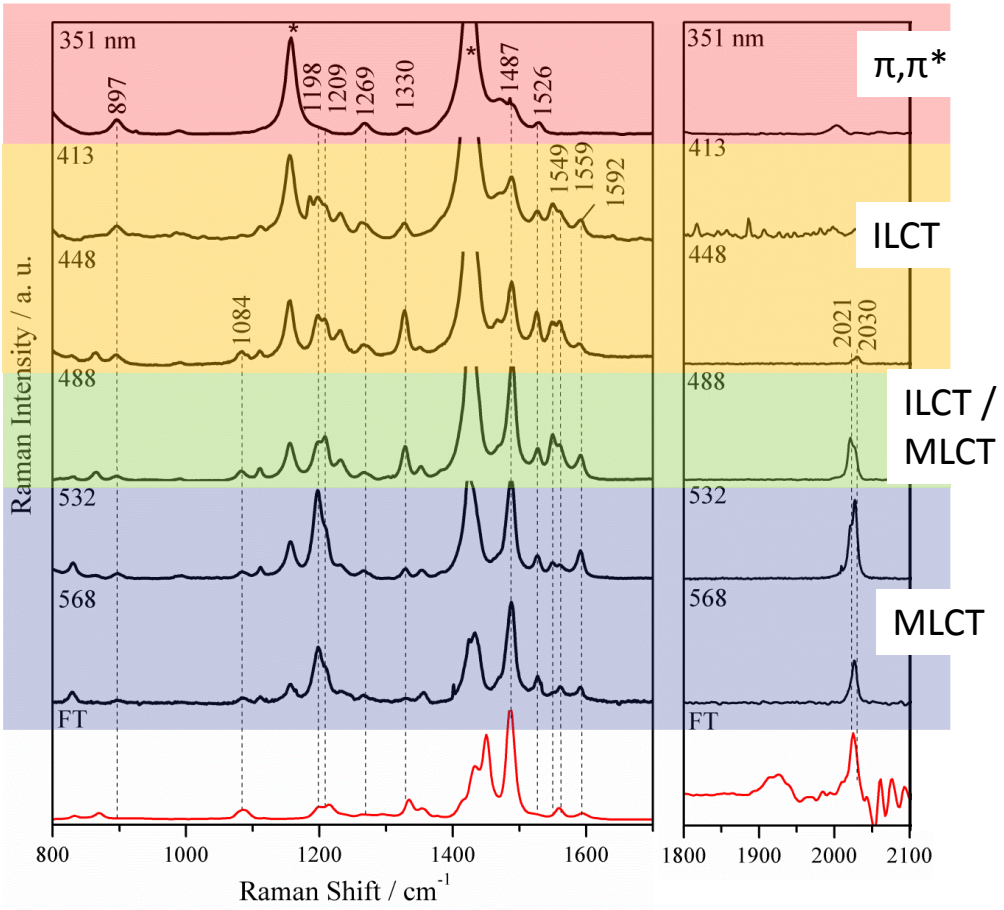

Figure 14. FT Raman (solid state) and Resonance Raman spectra of $(Re(CO)_3Cl)_3(\mu\text{-}HATN(SC_6H_{17})_6)$ in CH_2Cl_2. Enhancement patterns associated with LC π,π* (orange), ILCT (yellow), ILCT and MLCT (green) and MLCT (blue).

The enhancement of bands at 1330 cm^{-1} with excitation at 413 and 448 nm is consistent with an ILCT transition for S → HATN. With 488 nm excitation these bands show enhancement but in additionally carbonyl bands at 2021 and 2030 cm^{-1} are enhanced. These are both due to a'(1) bands of the carbonyls; the splitting occurs because different moieties may stretch in or out of phase with respect to each other.[42, 51, 82, 121] The enhancement of the a'(1) modes is consistent with an MLCT transition; however resonance Raman cannot differentiate between two overlapping transitions, i.e. ILCT and MLCT and a mixed transition. Time-resolved infrared on this system reveals that the oxidised rhenium centre shows a 31 cm^{-1} positive shift in $\Delta\tilde{\nu}$ (from 2020 to 2051 cm^{-1}). This is much less than for the non-sulfur system $(Re(CO)_3Cl)_3(\mu\text{-}HATN(CH_3)_6)$ in which the $\Delta\tilde{\nu}$ is 49 cm^{-1} (2024 to 2073 cm^{-1}). This provides unequivocal evidence of a mixed IL/MLCT transition corresponding to a concurrent partial oxidation of the metal and sulfur substituent.

The wider use of coupling chemistry has increased the range of substituents that can be appended to polypyridyl systems. The drive to panchromatic dyes, particularly in the field of DSSCs has seen the synthesis and study of a huge number of ligands and their respective ruthenium(II) complexes in which a variety of donor groups have been appended to the bipyridyl of phenanthroline ligands in order to increase absorption for the complexes and facilitate charge separation (*vide infra*).

5 Dye-sensitised solar cell systems

An important application for complexes with engineered ILCT and MLCT states is the dye-sensitized solar cells or DSSC, the mechanism of which has been reviewed.[1, 181, 182]. The basic processes are summarized in Figure 15. A dye is covalently bound to a thin mesoporous layer of sintered TiO_2 nanoparticles on top of a transparent conductive oxide layer on a glass substrate. A large surface area of the film is necessary in order to allow for a

high absorbance by the monolayer.[1] The first step in the mechanism is absorption of light by the dye, which causes excitation to an electronic excited state. This excited state may then inject an electron into the TiO_2 film (II) where it is transported (III) through the conductive oxide layer to perform work in an external circuit. The oxidized dye is then regenerated (V) by an electron donor such as iodide. The electron donor is regenerated by an electron from the counter electrode (typically triiodide is reduced to iodide). Processes which result in lower DSSC performance are shown with red arrows in (Figure 15). These include relaxation of the excited state (VI), back-electron transfer from the TiO_2 to regenerate the dye (VII) or external electron donor (VIII) and reduction of triiodide to iodide by the excited dye.

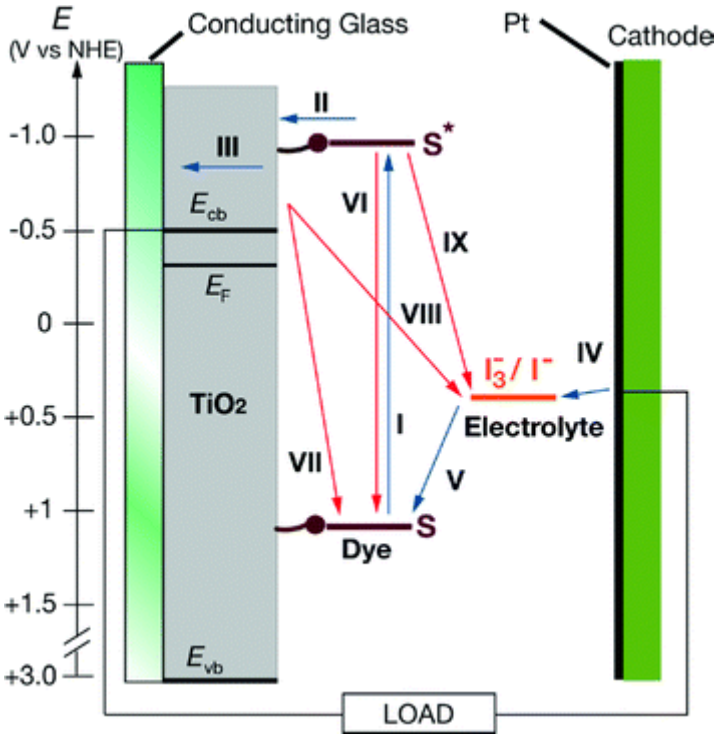

Figure 15: Summary of select processes in the DSSC. Processes I–V (blue arrows) ideally should be kinetically favoured over the recombination processes VI–IX (red arrows). (I) photoexcitation (II) electron-transfer from the dye to semiconductor; (III) electron-transport to the conducting glass through the film; (IV) reduction of iodide; (V) regeneration of the oxidized dye by the electrolyte species; (VI) radiative or non-radiative decay of the excited

dye; (VII) reduction of the oxidized dye by an electron from the semiconductor; (VIII) interception of electron from the semiconductor by triiodide (IX) reduction of electrolyte species by triiodide. Figure adapted from ref. [182] (used with permission from the Royal Society of Chemistry).

A dye for DSSCs should ideally be panchromatic, absorbing photons with a wavelength of 920 nm or shorter. It should also be strongly bound to the semiconductor surface and be stable enough to withstand redox turnovers for about 2 decades.[183] For many years the dye N719 was considered the "champion" DSSC dye. This complex builds upon $[Ru(bpy)_3]^{2+}$ by utilizing dcb (dcb = 4,4'-dicarboxy-2,2'-bipyridine) in place of two of the bpy ligands. The other bpy is replaced by a pair of thiocyanate ligands. Thiocyanate acts to increase the dπ energy level because of its strongly donating character. The carboxylate groups of the dcb ligands allow the complex to bind to the surface of the semiconductor particles.[1]

While development of better ruthenium dyes is still an active area of research, DSSCs utilizing organic dyes have also been developed which have efficiency on par with many metal complex based DSSCs. The structures of the dyes typically consist of an electron donor linked to an electron acceptor/anchor group. The donor group is often a coumarin or triarylamine (TAA) moiety. The anchor is typically cyanoacrylic acid which binds strongly to the TiO_2 surface. The donor is connected through a conjugated linker such as oligothiophene. The extinction coefficients of these dyes often approach an order of magnitude increase over classic Ru(II) dyes.[181]

There have been many attempts to merge organic chromophores with ruthenium dyes in order to achieve higher DSSC efficiencies.[1, 2] Aside from increasing the molar extinction coefficient of complexes, organic donor groups are also thought to increase DSSC efficiency

by helping to separate the electron-hole pair created upon photoexcitation and electron injection. In order to decrease the rate of back electron transfer to the oxidized dye a secondary electron donor can be covalently attached to the ruthenium complex. These are often called “super sensitizers" or antenna dyes. A simplified model of the mechanism is shown in equations A-C. Here the sensitizer (S) is covalently attached to the organic donor (D) and bound to TiO_2. The sensitizer is photoexcited and then becomes oxidized by the TiO_2. The dye is subsequently reduced by D. The recombination reaction (C) is slowed by presence of D because of the increased distance between D^+ and the nanoparticle surface.

$$\mathrm{D\text{–}S^*|TiO_2 \rightarrow D\text{–}S^+|TiO_2(e^-)} \quad \text{(A)}$$
$$\mathrm{D\text{–}S^+|TiO_2(e^-) \rightarrow D^+\text{–}S|TiO_2(e^-)} \quad \text{(B)}$$
$$\mathrm{D^+\text{–}S|TiO_2(e^-) \rightarrow D\text{–}S|TiO_2} \quad \text{(C)}$$

A pair of studies showed that triphenyl amine (TPA) donor groups could be attached to ligands of ruthenium dyes in order to increase hole separation, decrease the recombination rate and improve DSSC performance.[184, 185] Three heteroleptic complexes containing different numbers of amine groups were synthesized (Figure *16*). The first, $[Ru(dcb)_2(TPAbpy)]^{2+}$ contains two dcb ligands for anchoring the molecule to TiO_2 and a bpy ligand substituted with a TPA group on each pyridine ring through a conjugated ethenyl linker. The second complex, $[Ru(dcb)_2(TPDbpy)]^{2+}$ uses tetraphenyl benzidine (TPD) in place of TPA giving four amine donor groups. The third $[Ru(dcb)_2(poly\text{-}TPAbpy)]^{2+}$ used a bpy ligand attached to a TPA-based polymer giving roughly 100 amine donors per ruthenium core. TiO_2 films sensitized with these dyes were studied with nanosecond TA. Electron injection and oxidation of the amine component of the dyes occurs within the time resolution of the system but the kinetics of the back reaction could be observed. The half-time of the recombination process increases from 350 microseconds for $[Ru(dcb)_2(TPAbpy)]^{2+}$ to 4

seconds for $[Ru(dcb)_2(poly\text{-}TPAbpy)]^{2+}$ (4 orders of magnitude). This was attributed to an increase in the distance between the hole created on the amines and the TiO_2 surface. The data fit an electron tunnelling model where the rate constant for electron transfer has an exponential dependence on spatial separation.[184]

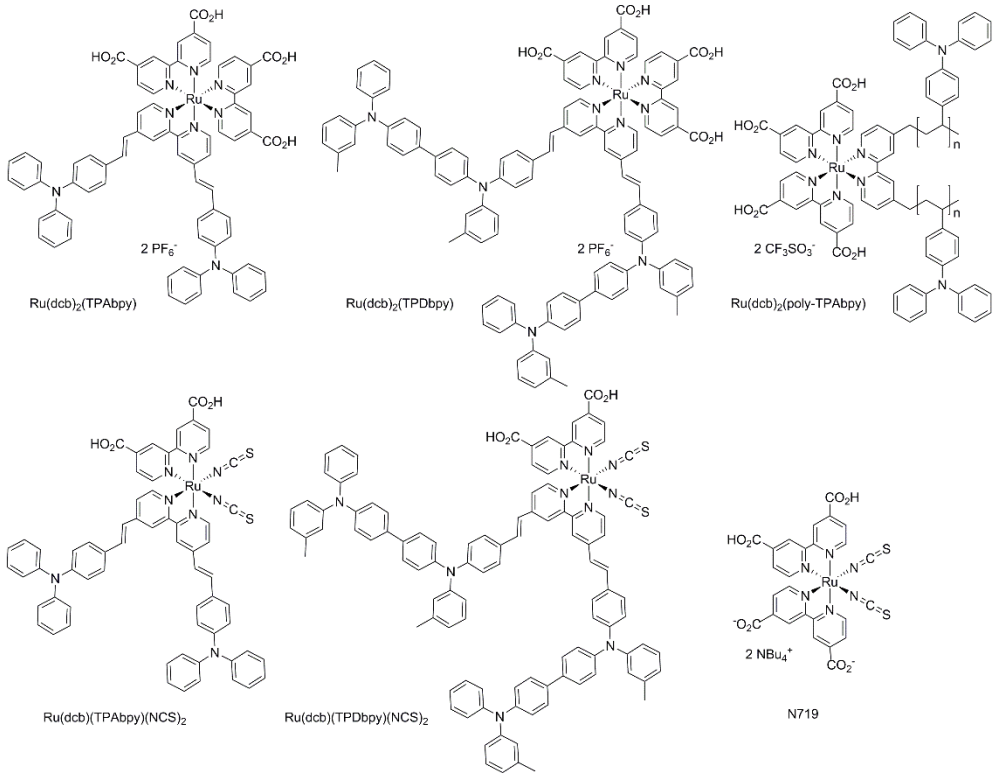

Figure 16 Solar cell dyes with TPA donor substituents and N719.[184, 185].

Modified Ru(II) complexes using the same TPAbpy and TPDbpy ligands in solid-state DSSC devices were later compared to the benchmark complex N719 (Figure *16*).[185] Replacement of one dcb ligand with a pair of NCS^- ligands gives analogues of N719 leaving two carboxylate groups remaining for binding the complex to TiO_2. The electronic absorption spectra of the complexes have a band at approximately the same wavelength as N719 which is assumed to be MLCT in nature. The slight increase in intensity and red-shift is attributed to increase conjugation length of the ligands TPAbpy and TPDbpy ligands compared to the dcb ligand of N719. Distinct strong absorption bands are also present at higher energy which

do not appear in the N719 spectrum. Performance of the devices increased by factors of 2 and 5 for [Ru(dcb)(TPAbpy)$(NCS)_2$] and [Ru(dcb)(TPDbpy)$(NCS)_2$] respectively over N719 under these conditions.

The increase in extinction coefficient in this class of complexes is often attributed to increased conjugation length compared to dcb. A multitude of N719 analogues with conjugated substituents have shown this to be the case. However it should be noted that TPA is an electron donor and this may give rise to distinct ILCT bands where the hole in the FC state is initially localized on the organic donor unit rather than the metal. Re (and Cu) complexes of the TPA-bpy ligand have been studied spectroscopically and computationally.[186] Although they may not be useful in solar cells they serve as model systems with close lying MLCT and ILCT states. The ILCT dominates the MLCT in the visible absorption band for the Re complex as shown with resonance Raman spectroscopy. TA and DFT show that the hole in the THEXI state is localized on the TPA units rather than the metal centre as in the Ru complex.

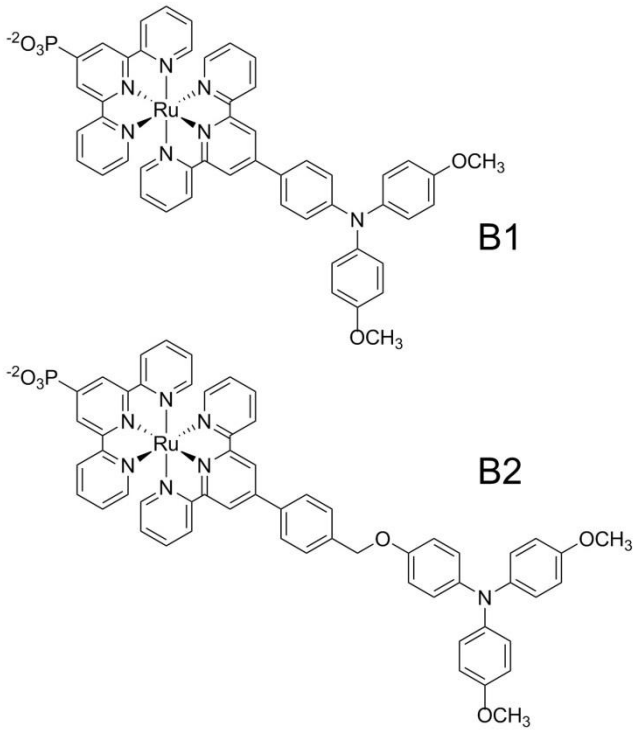

Figure 17. Complexes with TPA substituents and phosphate binders.[187]

In complexes such as [Ru(dcb)(TPAbpy)$(NCS)_2$] where two different π acceptor ligands are present (dcb and TPA-bpy) the energies of the π* orbitals of the two ligands becomes important for controlling interfacial charge separation and charge recombination. A comparison of two terpy-based ruthenium dads (Figure *17*) was performed by Bonhote and coworkers.[187] Both complexes use phosphate groups to bind to TiO_2 nanoparticle surfaces on one of the tridentate ligands (tpy-PO_3^{2-}). The other tridentate ligand is a phenyl-terpy ligand attached to TAA donor. The donor-substituted ligand is referred to as the proximal ligand and tpy-PO_3^{2-} is referred to as the distal ligand. In complex B1 there is conjugation between the TAA and the terpy portion of the proximal ligand opening the possibility of an ILCT band. In complex B2 a methoxy spacer prevents conjugation. Electronic absorption spectra show that complex B1 has red-shifted absorption with an increased molar extinction coefficient compared to B2 which would be expected to improve DSSC performance if no other factors were different.

The electron-transfer kinetics of the complexes bound to TiO_2 in propylene carbonate were compared using TA. For B1 only 60% of the excited molecules were found to undergo intramolecular electron transfer to form the oxidized TAA donor and an injected electron. For B2 the process was quantitative and recovery of the ground state was slower. This was attributed to differences in the localization of the lowest π^* orbital as determined by resonance Raman spectroscopy. Resonance Raman spectra show that for B1 the lowest absorption band predominantly involves the proximal ligand whereas in B2 it involves the distal ligand which is closer to the TiO_2 surface. This study showed that conjugation between the electron donor and chelating ligand can improve light harvesting but may have the unintended consequence of also lowering the π^* energy of the proximal ligand which can decrease electron injection efficiency.

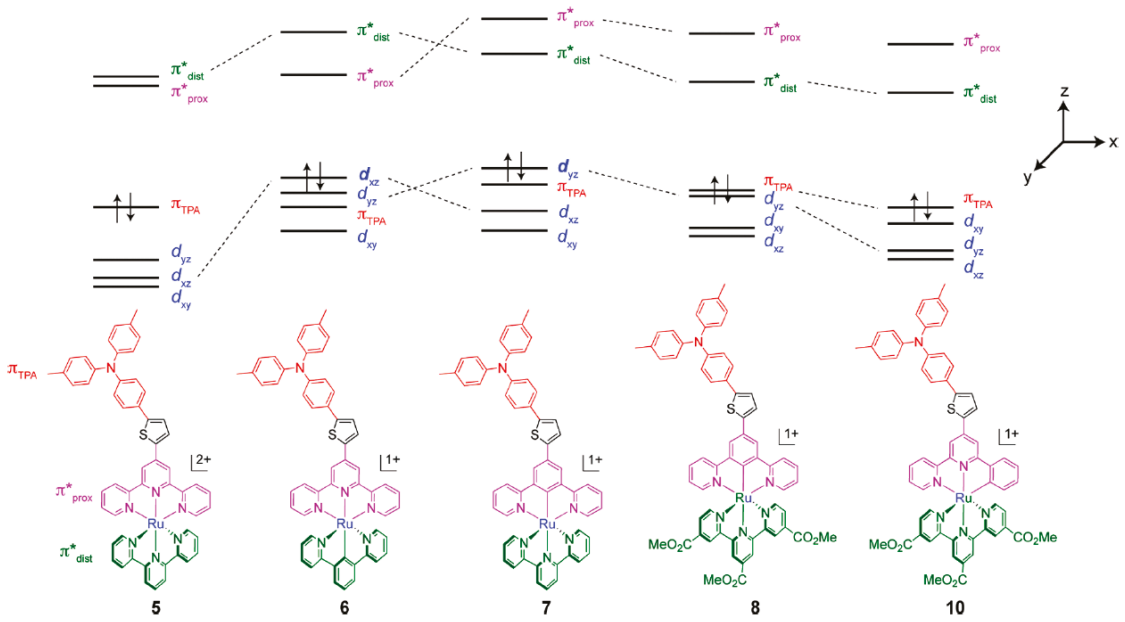

Figure 18 Qualitative energy level diagram showing the effects of cyclometallation on bis tridentate ruthenium dyes. Reprinted with permission from ref. [188]. Copyright (2011) American Chemical Society.

More recently several dyes which build upon dyad B1 have been synthesized and tested in DSSCs. Various conjugated groups were tested as linkers for the TAA and tpy on the proximal ligand. Thiophene was found to give complexes with the highest extinction coefficients [189], which was attributed to the presence of ILCT bands. Systematic studies of the effects of cyclometallation and TAA substituents on the energies of the dπ, π* and TAA π energy levels were performed (Figure 18).[182, 188] Cyclometallation could be used to tune the relative π* energy levels of the distal and proximal ligands, which also affects the dπ energy of Ru similarly to SCN^- ligands.[182] Some of the dyes were tested in DSSCs. As expected, the best performing complex was cyclometallated such that the distal ligand had a lower π* energy than the proximal ligand. The TAA unit was substituted with methoxy groups which ensure that it is more easily oxidized than the metal to facilitate hole transfer.

Despite the careful design of these complexes and their vastly improved visible absorption they still have lower performance in DSSCs compared to simpler dyes such as N719.

How can transient vibrational spectroscopy play a role in understanding types of complex systems? Recently complexes related to the dye N3, $[Ru(NCS)_2(dcb)_2]$ have been studied using transient methods and resonance Raman spectroscopy.[83] In order to improve the light absorbing abilities, the replacement of the COOH substituents at the 4,4'-positions of one or both of dcb ligands with extended conjugated moieties was performed. However, comparing $[Ru(NCS)_2(dcb)_2]$ to $[Ru(NCS)_2(dcb)(dxb)]$ (dxb is dpb = 4,4′-diphenylethenyl-bpy, dnb = 4,4′-dianthracenethenyl-bpy, dab = 4,4′-dinaphthylethenyl-bpy) shows little to no change in the lowest-energy absorption. Results from resonance Raman spectroscopy were found to be consistent with this and showed these transitions to be of the same character ($\{Ru(NCS)_2\} \rightarrow$ dcb). This could be explained by a small overlap of the acceptor MO with the conjugated substituents, which is in contrast to the studies presented above, where electron-donating substituents were appended. Higher energy excitation lead to absorption by the entire ligand, and obvious influences from the arene substituents were observed. It is possible that the use of different linkers, such as thiophene, would lead to more effective extension of conjugation. The excited states were investigated using TRIR and TR^2 (see Figure 19); for most complexes both techniques show a shift of $\tilde{\nu}$(NCS) of *ca.* -36 cm^{-1} (from 2109 to 2075 cm^{-1} for $[Ru(NCS)_2(dcb)_2]$). This is indicative of a reduction of electron density in the N=C=S bond, consistent with MLCT or ILCT excitation, as previously reported for N3. Other features in the TR^2 spectra appeared very similar to ground-state resonance Raman spectra acquired at λ_{ex} = 532 nm, with a slight increase in the relative intensity of the solvent bands. This may be due to very high NCS resonance enhancement in the excited state probed in addition to bleaching of the ground state. One exception is the TR^2 spectrum of $[Ru(NCS)_2(dcb)(dab)]$, which shows two bands in the $\tilde{\nu}$(NCS) region as well as several new

bands in the ligand stretching region (Figure 19). In TRIR, which provides time-resolution, the initially formed band at 2072 cm^{-1} can be seen to convert to a new band at 2099 cm^{-1}, which is only slightly shifted with respect to the ground state and persists for 150 ns. With the aid of excited state DFT calculations the new state was assigned as an anthracenyl to anthracenyl ILCT, similar to that observed for 9,9-bianthryl. The excited state in this case shows a significantly prolonged lifetime, which may be due to increased spatial separation compared to bianthryl.

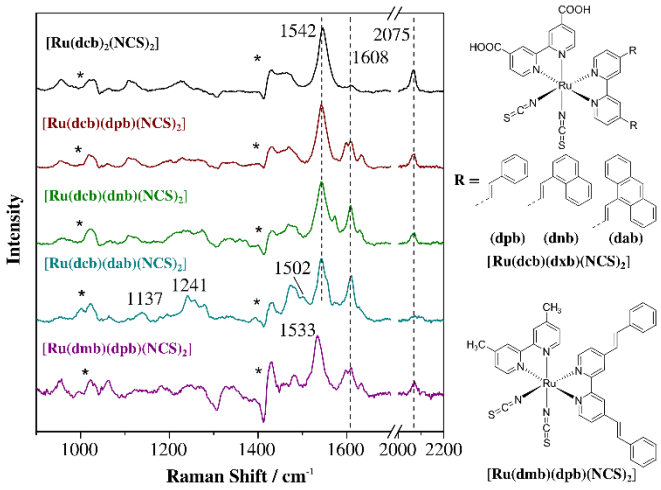

Figure 19. The TR^2 spectra of the ruthenium complexes, acquired in DMSO, with λ_{ex} = 532 nm. Vertical lines indicate common peaks throughout the series of complexes. Solvent peaks have been subtracted and residuals are marked with asterisks.

6 Conclusions

Inorganic photosystems have developed over the last decades to become increasingly electronically complex. The utility of this complexity has been used extensively in solar cells. Time-resolved vibrational spectroscopy with resonance Raman spectroscopy can be used to map the Franck-Condon to THEXI state relaxation processes through a variety of

excited state manifolds. These techniques can differentiate MLCT, LC and ILCT states and are capable of detecting different types of states within each of these broad classifications. The complexity of modern inorganic photosystems means that these methods are going to find increasing use in the determination of active excited states.

7 Acknowledgements

KCG and GJH acknowledge the support of the University of Otago and the MacDiarmid Institute.

8 References

[1] S. Ardo, G.J. Meyer, Chem. Soc. Rev., 38 (2009) 115--164.
[2] J.-F. Yin, M. Velayudham, D. Bhattacharya, H.-C. Lin, K.-L. Lu, Coord. Chem. Rev., 256 (2012) 3008--3035.
[3] K.K.W. Lo, K.Y. Zhang, S.P.Y. Li, European Journal of Inorganic Chemistry, (2011) 3551-3568.
[4] K.K.W. Lo, W.K. Hui, C.K. Chung, K.H.K. Tsang, T.K.M. Lee, C.K. Li, J.S.Y. Lau, D.C.M. Ng, Coordination Chemistry Reviews, 250 (2006) 1724-1736.
[5] Q. Zhao, F. Li, C. Huang, Chemical Society Reviews, 39 (2010) 3007-3030.
[6] Z. Ning, H. Tian, Chem. Commun., 2009 (2009) 5483.
[7] Y.-L. Rao, D. Schoenmakers, Y.-L. Chang, J.-S. Lu, Z.-H. Lu, Y. Kang, S. Wang, Chemistry, 18 (2012) 11306--11316.
[8] S.F. Sousa, R.N. Sampaio, N.M. Barbosa Neto, A.E.H. Machado, A.O.T. Patrocinio, Photochemical & Photobiological Sciences, 13 (2014) 1213-1224.
[9] G. Zhou, C.L. Ho, W.Y. Wong, Q. Wang, D. Ma, L. Wang, Z. Lin, T.B. Marder, A. Beeby, Adv. Funct. Mater., 18 (2008) 499--511.
[10] S. Sato, O. Ishitani, Coordination Chemistry Reviews, 282 (2015) 50-59.
[11] H. Takeda, O. Ishitani, Coordination Chemistry Reviews, 254 (2010) 346-354.
[12] C.D. Windle, M.W. George, R.N. Perutz, P.A. Summers, X.Z. Sun, A.C. Whitwood, Chemical Science, 6 (2015) 6847-6864.
[13] P.A. Summers, J.A. Calladine, F. Ghiotto, J. Dawson, X.-Z. Sun, M.L. Hamilton, M. Towrie, E.S. Davies, J. McMaster, M.W. George, M. Schröder, Inorganic Chemistry, (2015).
[14] M. Wachtler, J. Guthmuller, L. Gonzalez, B. Dietzek, Coordination Chemistry Reviews, 256 (2012) 1479-1508.
[15] A.W. Adamson, Journal of Chemical Education, 60 (1983) 797-802.
[16] S.M. Fredericks, J.C. Luong, M.S. Wrighton, J. Am. Chem. Soc., 101 (1979) 7415--7417.

[17] V. Skarda, M.J. Cook, A.P. Lewis, G.S.G. McAuliffe, A.J. Thomson, D.J. Robbins, J. Chem. Soc. Perkin Trans. 2, (1984) 1309.
[18] L.A. Worl, R. Duesing, P. Chen, L.D. Ciana, T.J. Meyer, J. Chem. Soc. Dalt. Trans., (1991) 849.
[19] P.A. Anderson, F.R. Keene, T.J. Meyer, J.A. Moss, G.F. Strouse, J.A. Treadway, Journal of the Chemical Society-Dalton Transactions, (2002) 3820-3831.
[20] J.A. Treadway, G.F. Strouse, R.R. Ruminski, T.J. Meyer, Inorganic Chemistry, 40 (2001) 4508-4509.
[21] D. Barpuzary, A. Banik, A.N. Panda, M. Qureshi, Journal of Physical Chemistry C, 119 (2015) 3892-3902.
[22] C. Goze, C. Leiggener, S.X. Liu, L. Sanguinet, E. Levillain, A. Hauser, S. Decurtins, Chemphyschem, 8 (2007) 1504-1512.
[23] N. Onozawa-Komatsuzaki, O. Kitao, M. Yanagida, Y. Himeda, H. Sugihara, K. Kasuga, New Journal of Chemistry, 30 (2006) 689-697.
[24] G. David, P.J. Walsh, K.C. Gordon, Chemical physics letters, 383 (2004) 292-296.
[25] N.J. Lundin, P.J. Walsh, S.L. Howell, A.G. Blackman, K.C. Gordon, Chemistry-a European Journal, 14 (2008) 11573-11583.
[26] N.J. Lundin, P.J. Walsh, S.L. Howell, J.J. McGarvey, A.G. Blackman, K.C. Gordon, Inorganic Chemistry, 44 (2005) 3551-3560.
[27] P.J. Walsh, K.C. Gordon, N.J. Lundin, A.G. Blackman, Journal of Physical Chemistry A, 109 (2005) 5933-5942.
[28] X.N. Li, Z.J. Wu, Z.J. Si, Z. Liang, X.J. Liu, H.J. Zhang, Physical Chemistry Chemical Physics, 11 (2009) 9687-9695.
[29] L.M. Zhang, B. Li, L.Y. Zhang, Z.M. Su, Acs Applied Materials & Interfaces, 1 (2009) 1852-1855.
[30] C.M. Dupureur, J.K. Barton, Inorganic Chemistry, 36 (1997) 33-43.
[31] A.E. Friedman, J.C. Chambron, J.P. Sauvage, N.J. Turro, J.K. Barton, Journal of the American Chemical Society, 112 (1990) 4960-4962.
[32] I. Haq, P. Lincoln, D.C. Suh, B. Norden, B.Z. Chowdhry, J.B. Chaires, Journal of the American Chemical Society, 117 (1995) 4788-4796.
[33] R.M. Hartshorn, J.K. Barton, Journal of the American Chemical Society, 114 (1992) 5919-5925.
[34] C. Hiort, P. Lincoln, B. Norden, Journal of the American Chemical Society, 115 (1993) 3448-3454.
[35] C.J. Murphy, M.R. Arkin, Y. Jenkins, N.D. Ghatlia, S.H. Bossmann, N.J. Turro, J.K. Barton, Science, 262 (1993) 1025-1029.
[36] E.R. Batista, R.L. Martin, Journal of Physical Chemistry A, 109 (2005) 3128-3133.
[37] L.Z. Hu, Z. Bian, H.J. Li, S. Han, Y.L. Yuan, L.X. Gao, G.B. Xu, Analytical Chemistry, 81 (2009) 9807-9811.
[38] A.W. McKinley, P. Lincoln, E.M. Tuite, Coordination Chemistry Reviews, 255 (2011) 2676-2692.
[39] H. Song, J.T. Kaiser, J.K. Barton, Nature Chemistry, 4 (2012) 615-620.
[40] J. Dyer, D.C. Grills, P. Matousek, A.W. Parker, M. Towrie, J.A. Weinstein, M.W. George, Chemical Communications, (2002) 872-873.
[41] M.K. Kuimova, D.C. Grills, P. Matousek, A.W. Parker, X.Z. Sun, M. Towrie, M.W. George, Vibrational Spectroscopy, 35 (2004) 219-223.
[42] M.K. Kuimova, K.C. Gordon, S.L. Howell, P. Matousek, A.W. Parker, X.Z. Sun, M. Towrie, M.W. George, Photochemical & Photobiological Sciences, 5 (2006) 82-87.

[43] J. Dyer, C.M. Creely, J.C. Penedo, D.C. Grills, S. Hudson, P. Matousek, A.W. Parker, M. Towrie, J.M. Kelly, M.W. George, Photochemical & Photobiological Sciences, 6 (2007) 741-748.
[44] M.K. Kuimova, W.Z. Alsindi, A.J. Blake, E.S. Davies, D.J. Lampus, P. Matousek, J. McMaster, A.W. Parker, M. Towrie, X.Z. Sun, C. Wilson, M.W. George, Inorganic Chemistry, 47 (2008) 9857-9869.
[45] Q. Cao, C.M. Creely, E.S. Davies, J. Dyer, T.L. Easun, D.C. Grills, D.A. McGovern, J. McMaster, J. Pitchford, J.A. Smith, X.Z. Sun, J.M. Kelly, M.W. George, Photochemical & Photobiological Sciences, 10 (2011) 1355-1364.
[46] E.D. Olmon, P.A. Sontz, A.M. Blanco-Rodriguez, M. Towrie, I.P. Clark, A. Vlcek, Jr., J.K. Barton, Journal of the American Chemical Society, 133 (2011) 13718-13730.
[47] R. Horvath, K.C. Gordon, Inorg. Chim. Acta, 374 (2011) 10-18.
[48] R.J.H. Clark, T.J. Dines, Angew. Chem. Int. Ed. Engl., 25 (1986) 131-158.
[49] R.L. McCreery, Raman Spectroscopy for Chemical Analysis, John Wiley & Sons, Inc., 2000.
[50] A.Y. Hirakawa, M. Tsuboi, Science (Washington, DC, United States), 188 (1975) 359-361.
[51] C.B. Larsen, H. van der Salm, C.A. Clark, A.B.S. Elliott, M.G. Fraser, R. Horvath, N.T. Lucas, X.-Z. Sun, M.W. George, K.C. Gordon, Inorganic Chemistry, 53 (2014) 1339-1354.
[52] M.G. Fraser, H. van der Salm, S.A. Cameron, J.E. Barnsley, K.C. Gordon, Polyhedron, 52 (2013) 623-633.
[53] L.C.T. Shoute, G.R. Loppnow, Journal of the American Chemical Society, 125 (2003) 15636-15646.
[54] W. Leng, F. Wuerthner, A.M. Kelley, Journal of Physical Chemistry B, 108 (2004) 10284-10294.
[55] S.L. Howell, K.C. Gordon, M.R. Waterland, K.H. Leung, D.L. Phillips, Journal of Physical Chemistry A, 110 (2006) 11194-11199.
[56] K.C. Gordon, J.J. McGarvey, Inorganic Chemistry, 30 (1991) 2986-2989.
[57] D.S. Egolf, M.R. Waterland, A.M. Kelley, Journal of Physical Chemistry B, 104 (2000) 10727-10737.
[58] M. Iwamura, S. Takeuchi, T. Tahara, Journal of the American Chemical Society, 129 (2007) 5248-5256.
[59] S.J. Lind, K.C. Gordon, M.R. Waterland, Journal of Raman Spectroscopy, 39 (2008) 1556-1567.
[60] J. Guthmuller, B. Champagne, Journal of Chemical Physics, 127 (2007).
[61] J. Guthmuller, B. Champagne, Chemphyschem, 9 (2008) 1667-1669.
[62] J. Guthmuller, B. Champagne, Journal of Physical Chemistry A, 112 (2008) 3215-3223.
[63] J. Guthmuller, B. Champagne, C. Moucheron, A. Kirsch-De Mesmaeker, Journal of Physical Chemistry B, 114 (2010) 511-520.
[64] J. Guthmuller, L. Gonzalez, Physical Chemistry Chemical Physics, 12 (2010) 14812-14821.
[65] S. Kupfer, J. Guthmuller, L. Gonzalez, Journal of Chemical Theory and Computation, 9 (2013) 543-554.
[66] S. Kupfer, J. Guthmuller, M. Wachtler, S. Losse, S. Rau, B. Dietzek, J. Popp, L. Gonzalez, Physical Chemistry Chemical Physics, 13 (2011) 15580-15588.
[67] S. Kupfer, M. Wachtler, J. Guthmuller, J. Popp, B. Dietzek, L. Gonzalez, Journal of Physical Chemistry C, 116 (2012) 19968-19977.
[68] F. Latorre, J. Guthmuller, P. Marquetand, Physical Chemistry Chemical Physics, 17 (2015) 7648-7658.

[69] C. Reichardt, M. Pinto, M. Wachtler, M. Stephenson, S. Kupfer, T. Sainuddin, J. Guthmuller, S.A. McFarland, B. Dietzek, Journal of Physical Chemistry A, 119 (2015) 3986-3994.
[70] J. Schindler, S. Kupfer, M. Wachtler, J. Guthmuller, S. Rau, B. Dietzek, Chemphyschem, 16 (2015) 1061-1070.
[71] M. Wachtler, J. Guthmuller, S. Kupfer, M. Maiuri, D. Brida, J. Popp, S. Rau, G. Cerullo, B. Dietzek, Chemistry-a European Journal, 21 (2015) 7668-7674.
[72] M. Wachtler, S. Kupfer, J. Guthmuller, J. Popp, L. Gonzalez, B. Dietzek, Journal of Physical Chemistry C, 115 (2011) 24004-24012.
[73] L. Zedler, J. Guthmuller, I.R. de Moraes, S. Kupfer, S. Krieck, M. Schmitt, J. Popp, S. Rau, B. Dietzek, Chemical Communications, 50 (2014) 5227-5229.
[74] Y. Zhang, S. Kupfer, L. Zedler, J. Schindler, T. Bocklitz, J. Guthmuller, S. Rau, B. Dietzek, Physical Chemistry Chemical Physics, 17 (2015) 29637-29646.
[75] J. Preiß, M. Jäger, S. Rau, B. Dietzek, J. Popp, T. Martínez, M. Presselt, ChemPhysChem, 16 (2015) 1395-1404.
[76] J.R. Schoonover, G.F. Strouse, R.B. Dyer, W.D. Bates, P.Y. Chen, T.J. Meyer, Inorganic Chemistry, 35 (1996) 273-&.
[77] M.W. George, J.J. Turner, Coordination Chemistry Reviews, 177 (1998) 201-217.
[78] M. Towrie, D.C. Grills, J. Dyer, J.A. Weinstein, P. Matousek, R. Barton, P.D. Bailey, N. Subramaniam, W.M. Kwok, C. Ma, D. Phillips, A.W. Parker, M.W. George, Applied Spectroscopy, 57 (2003) 367-380.
[79] G.M. Greetham, P. Burgos, Q. Cao, I.P. Clark, P.S. Codd, R.C. Farrow, M.W. George, M. Kogimtzis, P. Matousek, A.W. Parker, M.R. Pollard, D.A. Robinson, Z.-J. Xin, M. Towrie, Applied Spectroscopy, 64 (2010) 1311-1319.
[80] Y. Yue, T. Grusenmeyer, Z. Ma, P. Zhang, T.T. Pham, J.T. Mague, J.P. Donahue, R.H. Schmehl, D.N. Beratan, I.V. Rubtsov, Journal of Physical Chemistry B, 117 (2013) 15903-15916.
[81] J.A. Calladine, R. Horvath, A.J. Davies, A. Wriglesworth, X.Z. Sun, M.W. George, Applied Spectroscopy, 69 (2015) 519-524.
[82] M.G. Fraser, C.A. Clark, R. Horvath, S.J. Lind, A.G. Blackman, X.-Z. Sun, M.W. George, K.C. Gordon, Inorganic Chemistry, 50 (2011) 6093-6106.
[83] R. Horvath, M.G. Fraser, C.A. Clark, X.-Z. Sun, M.W. George, K.C. Gordon, Inorganic Chemistry, (2015).
[84] K. Takeshita, Y. Sasaki, M. Kobashi, Y. Tanaka, S. Maeda, A. Yamakata, T. Ishibashi, H. Onishi, J. Phys. Chem. B, 107 (2003) 4156-4161.
[85] J.B. Asbury, R.J. Ellingson, H.N. Ghosh, S. Ferrere, A.J. Nozik, T. Lian, J. Phys. Chem. B, 103 (1999) 3110-3119.
[86] J.B. Asbury, E. Hao, Y. Wang, T. Lian, J. Phys. Chem. B, 104 (2000) 11957-11964.
[87] J.B. Asbury, E. Hao, Y. Wang, H.N. Ghosh, T. Lian, J. Phys. Chem. B, 105 (2001) 4545-4557.
[88] W. Chen, C. Turro, L.A. Friedman, J.K. Barton, N.J. Turro, Journal of Physical Chemistry B, 101 (1997) 6995-7000.
[89] M. Delor, T. Keane, P.A. Scattergood, I.V. Sazanovich, G.M. Greetham, M. Towrie, A.J.H.M. Meijer, J.A. Weinstein, Nat Chem, 7 (2015) 689-695.
[90] M. Delor, P.A. Scattergood, I.V. Sazanovich, A.W. Parker, G.M. Greetham, A.J.H.M. Meijer, M. Towrie, J.A. Weinstein, Science, 346 (2014) 1492-1495.
[91] J.M. Butler, M.W. George, J.R. Schoonover, D.M. Dattelbaum, T.J. Meyer, Coordination Chemistry Reviews, 251 (2007) 492-514.
[92] J. Bredenbeck, J. Helbing, P. Hamm, Journal of the American Chemical Society, 126 (2004) 990-991.

[93] J. Dyer, W.J. Blau, C.G. Coates, C.M. Creely, J.D. Gavey, M.W. George, D.C. Grills, S. Hudson, J.M. Kelly, P. Matousek, J.J. McGarvey, J. McMaster, A.W. Parker, M. Towrie, J.A. Weinstein, Photochemical & Photobiological Sciences, 2 (2003) 542-554.
[94] R. Horvath, C.A. Otter, K.C. Gordon, A.M. Brodie, E.W. Ainscough, Inorganic Chemistry, 49 (2010) 4073-4083.
[95] D.S. Caswell, T.G. Spiro, Inorganic Chemistry, 26 (1987) 18-22.
[96] K.C. Gordon, J.J. McGarvey, Chemical Physics Letters, 173 (1990) 443-448.
[97] M. Forster, R.E. Hester, Chemical Physics Letters, 81 (1981) 42-47.
[98] R.F. Dallinger, W.H. Woodruff, Journal of the American Chemical Society, 101 (1979) 4391-4393.
[99] P.G. Bradley, N. Kress, B.A. Hornberger, R.F. Dallinger, W.H. Woodruff, Journal of the American Chemical Society, 103 (1981) 7441-7446.
[100] C. Turro, Y.C. Chung, N. Leventis, M.E. Kuchenmeister, P.J. Wagner, G.E. Leroi, Inorganic Chemistry, 35 (1996) 5104-&.
[101] K.M. Omberg, J.R. Schoonover, S. Bernhard, J.A. Moss, J.A. Treadway, E.M. Kober, R.B. Dyer, T.J. Meyer, Inorganic Chemistry, 37 (1998) 3505-3508.
[102] J.R. Schoonover, K.M. Omberg, J.A. Moss, S. Bernhard, V.J. Malueg, W.H. Woodruff, T.J. Meyer, Inorganic Chemistry, 37 (1998) 2585-2587.
[103] C.G. Coates, T.E. Keyes, J.J. McGarvey, H.P. Hughes, J.G. Vos, P.M. Jayaweera, Coordination Chemistry Reviews, 171 (1998) 323-330.
[104] W. Henry, C.G. Coates, C. Brady, K.L. Ronayne, P. Matousek, M. Towrie, S.W. Botchway, A.W. Parker, J.G. Vos, W.R. Browne, J.J. McGarvey, Journal of Physical Chemistry A, 112 (2008) 4537-4544.
[105] D.J. Liard, M. Busby, I.R. Farrell, P. Matousek, M. Towrie, A. Vlcek, Journal of Physical Chemistry A, 108 (2004) 556-567.
[106] D.J. Liard, M. Busby, P. Matousek, M. Towrie, A. Vlcek, Journal of Physical Chemistry A, 108 (2004) 2363-2369.
[107] D.J. Liard, C.J. Kleverlaan, A. Vlcek, Inorganic Chemistry, 42 (2003) 7995-8002.
[108] V.R.L. Constantino, H.E. Toma, I.F.C. Deoliveira, P.S. Santos, Journal of Raman Spectroscopy, 23 (1992) 629-632.
[109] J.S. Gardner, D.P. Strommen, W.S. Szulbinski, H.Q. Su, J.R. Kincaid, Journal of Physical Chemistry A, 107 (2003) 351-357.
[110] I. Ortmans, P. Didier, A. Kirschdemesmaeker, Inorganic Chemistry, 34 (1995) 3695-3704.
[111] J.R. Schoonover, P.Y. Chen, W.D. Bates, R.B. Dyer, T.J. Meyer, Inorganic Chemistry, 33 (1994) 793-797.
[112] C. Turro, S.H. Bossmann, G.E. Leroi, J.K. Barton, N.J. Turro, Inorganic Chemistry, 33 (1994) 1344-1347.
[113] D.J. Manuel, D.P. Strommen, A. Bhuiyan, M. Sykora, J.R. Kincaid, Journal of Raman Spectroscopy, 28 (1997) 933-938.
[114] H.Q. Su, J.R. Kincaid, Journal of Raman Spectroscopy, 34 (2003) 907-916.
[115] W.S. Szulbinski, J.R. Kincaid, Inorganic Chemistry, 37 (1998) 859-864.
[116] J. Wu, J.R. Kincaid, Journal of Raman Spectroscopy, 35 (2004) 1001-1005.
[117] A. Gabrielsson, M. Towrie, S. Záliš, A. Vlček, Inorganic Chemistry, 47 (2008) 4236-4242.
[118] H.A. Nieuwenhuis, D.J. Stufkens, R.A. McNicholl, A.H.R. Alobaidi, C.G. Coates, S.E.J. Bell, J.J. McGarvey, J. Westwell, M.W. George, J.J. Turner, Journal of the American Chemical Society, 117 (1995) 5579-5585.
[119] B.D. Rossenaar, D.J. Stufkens, A. Vlcek, Inorganic Chemistry, 35 (1996) 2902-2909.

[120] H.A. Nieuwenhuis, D.J. Stufkens, A. Vlcek, Inorganic Chemistry, 34 (1995) 3879-3886.
[121] L.C. Abbott, C.J. Arnold, T.Q. Ye, K.C. Gordon, R.N. Perutz, R.E. Hester, J.N. Moore, Journal of Physical Chemistry A, 102 (1998) 1252-1260.
[122] M.W. George, F.P.A. Johnson, J.R. Westwell, P.M. Hodges, J.J. Turner, Journal of the Chemical Society-Dalton Transactions, (1993) 2977-2979.
[123] I.E. Pomestchenko, D.E. Polyansky, F.N. Castellano, Inorganic Chemistry, 44 (2005) 3412-3421.
[124] D.R. Gamelin, M.W. George, P. Glyn, F.-W. Grevels, F.P.A. Johnson, W. Klotzbuecher, S.L. Morrison, G. Russell, K. Schaffner, J.J. Turner, Inorganic Chemistry, 33 (1994) 3246-3250.
[125] M.K. Kuimova, W.Z. Alsindi, J. Dyer, D.C. Grills, O.S. Jina, P. Matousek, A.W. Parker, P. Portius, X. Zhong Sun, M. Towrie, C. Wilson, J. Yang, M.W. George, Dalton Transactions, (2003) 3996-4006.
[126] A. El Nahhas, C. Consani, A.M. Blanco-Rodriguez, K.M. Lancaster, O. Braem, A. Cannizzo, M. Towrie, I.P. Clark, S. Zalis, M. Chergui, A. Vlcek, Jr., Inorganic Chemistry, 50 (2011) 2932-2943.
[127] T.Y. Kim, A.B.S. Elliott, K.J. Shaffer, C.J. McAdam, K.C. Gordon, J.D. Crowley, Polyhedron, 52 (2013) 1391-1398.
[128] C.B. Anderson, A.B.S. Elliott, C.J. McAdam, K.C. Gordon, J.D. Crowley, Organometallics, 32 (2013) 788-797.
[129] S.M. McNeill, D. Preston, J.E.M. Lewis, A. Robert, K. Knerr-Rupp, D.O. Graham, J.R. Wright, G.I. Giles, J.D. Crowley, Dalton Transactions, 44 (2015) 11129-11136.
[130] J.E.M. Lewis, A.B.S. Elliott, C.J. McAdam, K.C. Gordon, J.D. Crowley, Chemical Science, 5 (2014) 1833-1843.
[131] A.M. Blanco-Rodriguez, H. Kvapilova, J. Sykora, M. Towrie, C. Nervi, G. Volpi, S. Zalis, A. Vlcek, Jr., Journal of the American Chemical Society, 136 (2014) 5963-5973.
[132] S.E. Brown-Xu, M.H. Chisholm, C.B. Durr, T.L. Gustafson, T.F. Spilker, Journal of Physical Chemistry A, 117 (2013) 5997-6006.
[133] L.D. Movsisyan, M.D. Peeks, G.M. Greetham, M. Towrie, A.L. Thompson, A.W. Parker, H.L. Anderson, Journal of the American Chemical Society, 136 (2014) 17996-18008.
[134] A.M. Blanco-Rodriguez, M. Busby, C. Gradinaru, B.R. Crane, A.J. Di Bilio, P. Matousek, M. Towrie, B.S. Leigh, J.H. Richards, A. Vlcek, H.B. Gray, Journal of the American Chemical Society, 128 (2006) 4365-4370.
[135] M. Busby, A. Gabrielsson, P. Matousek, M. Towrie, A.J. Di Bilio, H.B. Gray, A. Vlcek, Inorganic Chemistry, 43 (2004) 4994-5002.
[136] C. Shih, A.K. Museth, M. Abrahamsson, A.M. Blanco-Rodriguez, A.J. Di Bilio, J. Sudhamsu, B.R. Crane, K.L. Ronayne, M. Towrie, A. Vlček, J.H. Richards, J.R. Winkler, H.B. Gray, Science, 320 (2008) 1760-1762.
[137] A.M. Blanco-Rodriguez, M. Busby, K. Ronayne, M. Towrie, C. Gradinaru, J. Sudhamsu, J. Sykora, M. Hof, S. Zalis, A.J. Di Bilio, B.R. Crane, H.B. Gray, A. Vlcek, Jr., Journal of the American Chemical Society, 131 (2009) 11788-11800.
[138] A.M. Blanco-Rodriguez, A.J. Di Bilio, C. Shih, A.K. Museth, I.P. Clark, M. Towrie, A. Cannizzo, J. Sudhamsu, B.R. Crane, J. Sykora, J.R. Winkler, H.B. Gray, S. Zalis, A. Vlcek, Jr., Chem. Eur. J., 17 (2011) 5350-5361.
[139] A.M. Blanco Rodríguez, A. Gabrielsson, M. Motevalli, P. Matousek, M. Towrie, J. Šebera, S. Záliš, A. Vlček, The Journal of Physical Chemistry A, 109 (2005) 5016-5025.
[140] D.M. Dattelbaum, M.K. Itokazu, N.Y.M. Iha, T.J. Meyer, Journal of Physical Chemistry A, 107 (2003) 4092-4095.

[141] D.M. Dattelbaum, K.M. Omberg, P.J. Hay, N.L. Gebhart, R.L. Martin, J.R. Schoonover, T.J. Meyer, Journal of Physical Chemistry A, 108 (2004) 3527-3536.
[142] M. Busby, P. Matousek, M. Towrie, A. Vlcek, Journal of Physical Chemistry A, 109 (2005) 3000-3008.
[143] Y. Yue, T. Grusenmeyer, Z. Ma, P. Zhang, R.H. Schmeht, D.N. Beratan, I.V. Rubtsov, Journal of Physical Chemistry A, 118 (2014) 10407-10415.
[144] B. Elias, C. Creely, G.W. Doorley, M.M. Feeney, C. Moucheron, A. Kirsch-DeMesmaeker, J. Dyer, D.C. Grills, M.W. George, P. Matousek, A.W. Parker, M. Towrie, J.M. Kelly, Chemistry-a European Journal, 14 (2008) 369-375.
[145] M.R. Waterland, K.C. Gordon, J.J. McGarvey, P.M. Jayaweera, Journal of the Chemical Society-Dalton Transactions, (1998) 609-616.
[146] B.J. Matthewson, A. Flood, M.I.J. Polson, C. Armstrong, D.L. Phillips, K.C. Gordon, Bulletin of the Chemical Society of Japan, 75 (2002) 933-942.
[147] B. Schafer, H. Goerls, M. Presselt, M. Schmitt, J. Popp, W. Henry, J.G. Vos, S. Rau, Dalton Transactions, (2006) 2225-2231.
[148] C. Kuhnt, M. Karnahl, S. Tschierlei, K. Griebenow, M. Schmitt, B. Schafer, S. Krieck, H. Gorls, S. Rau, B. Dietzek, J. Popp, Physical Chemistry Chemical Physics, 12 (2010) 1357-1368.
[149] M.R. Waterland, K.C. Gordon, Journal of Raman Spectroscopy, 31 (2000) 243-253.
[150] N.J. Lundin, A.G. Blackman, K.C. Gordon, D.L. Officer, Angewandte Chemie International Edition, 45 (2006) 2582-2584.
[151] C.G. Coates, P. Callaghan, J.J. McGarvey, J.M. Kelly, L. Jacquet, A. Kirsch-De Mesmaeker, Journal of Molecular Structure, 598 (2001) 15-25.
[152] M.K. Brennaman, J.H. Alstrum-Acevedo, C.N. Fleming, P. Jang, T.J. Meyer, J.M. Papanikolas, Journal of the American Chemical Society, 124 (2002) 15094-15098.
[153] M.K. Brennaman, T.J. Meyer, J.M. Papanikolas, Journal of Physical Chemistry A, 108 (2004) 9938-9944.
[154] M.K. Kuimova, X.Z. Sun, P. Matousek, D.C. Grills, A.W. Parker, M. Towrie, M.W. George, Photochemical & Photobiological Sciences, 6 (2007) 1158-1163.
[155] M.B. Majewski, N.R. de Tacconi, F.M. MacDonnell, M.O. Wolf, Chemistry-a European Journal, 19 (2013) 8331-8341.
[156] M. Brautigam, M. Wachtler, S. Rau, J. Popp, B. Dietzek, Journal of Physical Chemistry C, 116 (2012) 1274-1281.
[157] H. van der Salm, M.G. Fraser, R. Horvath, S.A. Cameron, J.E. Barnsley, X.Z. Sun, M.W. George, K.C. Gordon, Inorganic Chemistry, 53 (2014) 3126-3140.
[158] C. Kuhnt, S. Tschierlei, M. Karnahl, S. Rau, B. Dietzek, M. Schmitt, J. Popp, Journal of Raman Spectroscopy, 41 (2010) 922-932.
[159] H. van der Salm, C.B. Larsen, J.R.W. McLay, M.G. Fraser, N.T. Lucas, K.C. Gordon, Dalton Transactions, 43 (2014) 17775-17785.
[160] J.A. Smith, M.W. George, J.M. Kelly, Coordination Chemistry Reviews, 255 (2011) 2666-2675.
[161] M. Towrie, G.W. Doorley, M.W. George, A.W. Parker, S.J. Quinn, J.M. Kelly, Analyst, 134 (2009) 1265-1273.
[162] C.G. Coates, L. Jacquet, J.J. McGarvey, S.E.J. Bell, A.H.R. AlObaidi, J.M. Kelly, Chemical Communications, (1996) 35-36.
[163] C.G. Coates, L. Jacquet, J.J. McGarvey, S.E.J. Bell, A.H.R. AlObaidi, J.M. Kelly, Journal of the American Chemical Society, 119 (1997) 7130-7136.
[164] P.M. Keane, F.E. Poynton, J.P. Hall, I.P. Clark, I.V. Sazanovich, M. Towrie, T. Gunnlaugsson, S.J. Quinn, C.J. Cardin, J.M. Kelly, The Journal of Physical Chemistry Letters, 6 (2015) 734-738.

[165] J.P. Hall, F.E. Poynton, P.M. Keane, S.P. Gurung, J.A. Brazier, D.J. Cardin, G. Winter, T. Gunnlaugsson, I.V. Sazanovich, M. Towrie, C.J. Cardin, J.M. Kelly, S.J. Quinn, Nat Chem, 7 (2015) 961-967.
[166] S.J. Devereux, P.M. Keane, S. Vasudevan, I.V. Sazanovich, M. Towrie, Q. Cao, X.-Z. Sun, M.W. George, C.J. Cardin, N.A.P. Kane-Maguire, J.M. Kelly, S.J. Quinn, Dalton Transactions, 43 (2014) 17606-17609.
[167] D.S. Tyson, F.N. Castellana, Inorganic Chemistry, 38 (1999) 4382-+.
[168] D.S. Tyson, F.N. Castellano, Journal of Physical Chemistry A, 103 (1999) 10955-10960.
[169] D.S. Tyson, J. Bialecki, F.N. Castellano, Chemical Communications, (2000) 2355-2356.
[170] D.S. Tyson, I. Gryczynski, F.N. Castellano, Journal of Physical Chemistry A, 104 (2000) 2919-2924.
[171] X.L. Zhou, D.S. Tyson, F.N. Castellano, Angewandte Chemie-International Edition, 39 (2000) 4301-+.
[172] D.S. Tyson, C.R. Luman, X.L. Zhou, F.N. Castellano, Inorganic Chemistry, 40 (2001) 4063-4071.
[173] D.S. Tyson, K.B. Henbest, J. Bialecki, F.N. Castellano, Journal of Physical Chemistry A, 105 (2001) 8154-8161.
[174] D.S. Tyson, C.R. Luman, F.N. Castellano, Inorganic Chemistry, 41 (2002) 3578-3586.
[175] C. Goze, D.V. Kozlov, D.S. Tyson, R. Ziessel, F.N. Castellano, New Journal of Chemistry, 27 (2003) 1679-1683.
[176] D.V. Kozlov, D.S. Tyson, C. Goze, R. Ziessel, F.N. Castellano, Inorganic Chemistry, 43 (2004) 6083-6092.
[177] D.E. Polyansky, E.O. Danilov, F.N. Castellano, Inorganic Chemistry, 45 (2006) 2370-2372.
[178] J.E. Yarnell, J.C. Deaton, C.E. McCusker, F.N. Castellano, Inorganic Chemistry, 50 (2011) 7820-7830.
[179] M.G. Fraser, A.G. Blackman, G.I.S. Irwin, C.P. Easton, K.C. Gordon, Inorganic Chemistry, 49 (2010) 5180-5189.
[180] H. van der Salm, M.G. Fraser, R. Horvath, J.O. Turner, G.M. Greetham, I.P. Clark, M. Towrie, N.T. Lucas, M.W. George, K.C. Gordon, Inorganic Chemistry, 53 (2014) 13049-13060.
[181] A. Mishra, M.K.R. Fischer, P. Buerle, Angew. Chemie Int. Ed., 48 (2009) 2474--2499.
[182] K.C.D. Robson, P.G. Bomben, C.P. Berlinguette, Dalt. Trans., 41 (2012) 7814.
[183] M.K. Nazeeruddin, P. Péchy, T. Renouard, S.M. Zakeeruddin, R. Humphry-Baker, P. Comte, P. Liska, L. Cevey, E. Costa, V. Shklover, L. Spiccia, G.B. Deacon, C.A. Bignozzi, M. Grätzel, Journal of the American Chemical Society, 123 (2001) 1613-1624.
[184] S.A. Haque, S. Handa, K. Peter, E. Palomares, M. Thelakkat, J.R. Durrant, Angew. Chem. Int. Ed. Engl., 44 (2005) 5740--5744.
[185] C.S. Karthikeyan, H. Wietasch, M. Thelakkat, Adv. Mater., 19 (2007) 1091--1095.
[186] R. Horvath, M.G. Fraser, S.A. Cameron, A.G. Blackman, P. Wagner, D.L. Officer, K.C. Gordon, Inorg. Chem., 52 (2013) 1304--1317.
[187] P. Bonhte, J.E. Moser, R. Humphry-Baker, N. Vlachopoulos, S.M. Zakeeruddin, L. Walder, M. Grtzel, J. Am. Chem. Soc., 121 (1999) 1324--1336.
[188] K.C.D. Robson, B.D. Koivisto, A. Yella, B. Sporinova, M.K. Nazeeruddin, T. Baumgartner, M. Grätzel, C.P. Berlinguette, Inorganic Chemistry, 50 (2011) 5494-5508.
[189] K.C.D. Robson, B.D. Koivisto, T.J. Gordon, T. Baumgartner, C.P. Berlinguette, Inorg. Chem., 49 (2010) 5335--5337.